# 3N reactions with chiral $N^3LO$ forces

**H. Witała**
**Jagiellonian University, Kraków**

**in collaboration with:**

**J. Golak, R. Skibiński, K. Topolnicki, Kraków**

**E. Epelbaum, H. Krebs, Bochum University**

**W.N. Polyzou, the University of Iowa**

**A. Nogga, Forschungszentrum Juelich**

**H. Kamada, Kyushu Institute of Technology**

- **Low energies:** $N^3LO$ NN + 3NF and $A_y$ puzzle

- **How good we know low energy nn $^1S_0$ force:** Dineutron and nd observables

- **Higher energies:** 3NF and relativistic effects

# Introduction – 2N and 3N systems

- Nonrelativistic formalism
- 2N:

  Schrödinger equation,

  Lippmann-Schwinger equation for the t-matrix

  (interaction + free propagation)

$$t(E) = V + VG_0(E)V + VG_0VG_0(E)V + \ldots$$

$$G_0(E) \equiv \lim_{\varepsilon \to 0^+} \frac{1}{E - H_0 + i\varepsilon}$$

- 3N: Faddeev equation

$$T = tP\phi + (1+tG_0)V_{123}^{(1)}(1+P)\phi + tPG_0T + (1+tG_0)V_{123}^{(1)}(1+P)G_0T$$

Transition amplitudes

$$U = PG_0^{-1} + V_{123}^{(1)}(1+P)\phi +$$

$$+ PT + V_{123}^{(1)}(1+P)G_0T$$

$$U_0 = (1+P)T$$

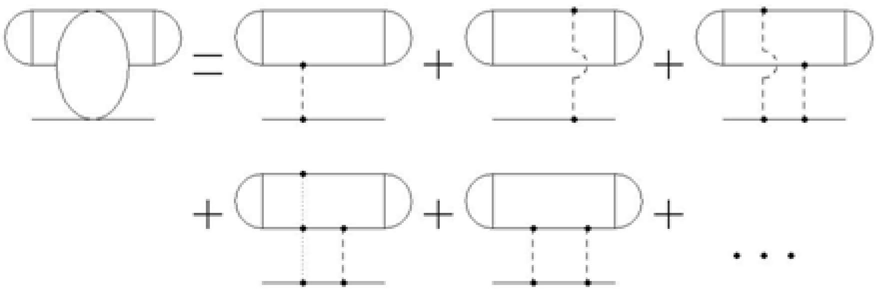

# Introduction – 2N and 3N systems

- Input to those equations is:

- the nucleon-nucleon potential V (CD Bonn, AV18, Nijm, chiral)
- the three nucleon force $V_{123}$ (TM, Urbana IX, chiral)

Solutions allow us to calculate properties of $^3H$ and $^3He$ and different observables in elastic NN and Nd scattering and in the deuteron breakup reaction.

# To describe 2N system it is necessary and sufficient to go to $N^3LO$ in chiral expansion:

- E. Epelbaum, H. -W. Hammer, U.-G. Meißner, Rev. Mod. Phys. 81, 1773 (2009)
- R. Machleidt, D. R. Entem, Phys. Rept. 503, 1 (2011)

| Potential | LS cut-off [MeV] | SFR cut-off [MeV] | $E_d$ [MeV] | $P_d$ [%] |
|---|---|---|---|---|
| N2LO 101 | 450 | 500 | -2.1922 | 3.536 |
| N2LO 102 | 600 | 500 | -2.1842 | 4.566 |
| N2LO 103 | 550 | 600 | -2.1887 | 4.383 |
| N2LO 104 | 450 | 700 | -2.2019 | 3.613 |
| N2LO 105 | 600 | 700 | -2.1997 | 4.709 |
| N3LO 201 | 450 | 500 | -2.2161 | 2.727 |
| N3LO 202 | 600 | 600 | -2.2212 | 3.545 |
| N3LO 203 | 550 | 600 | -2.2193 | 3.283 |
| N3LO 204 | 450 | 700 | -2.2187 | 2.844 |
| N3LO 205 | 600 | 700 | -2.2232 | 3.634 |

TABLE I: The cut-off's for Lippmann-Schwinger eq. (LS) regularization and spectral function regularization (SFR) together with the deuteron properties (E. Epelbaum Prog. Part. Nucl. Phys. **57**, 654 (2006)).

# Various topologies contributing to the 3NF up to and including N$^4$LO

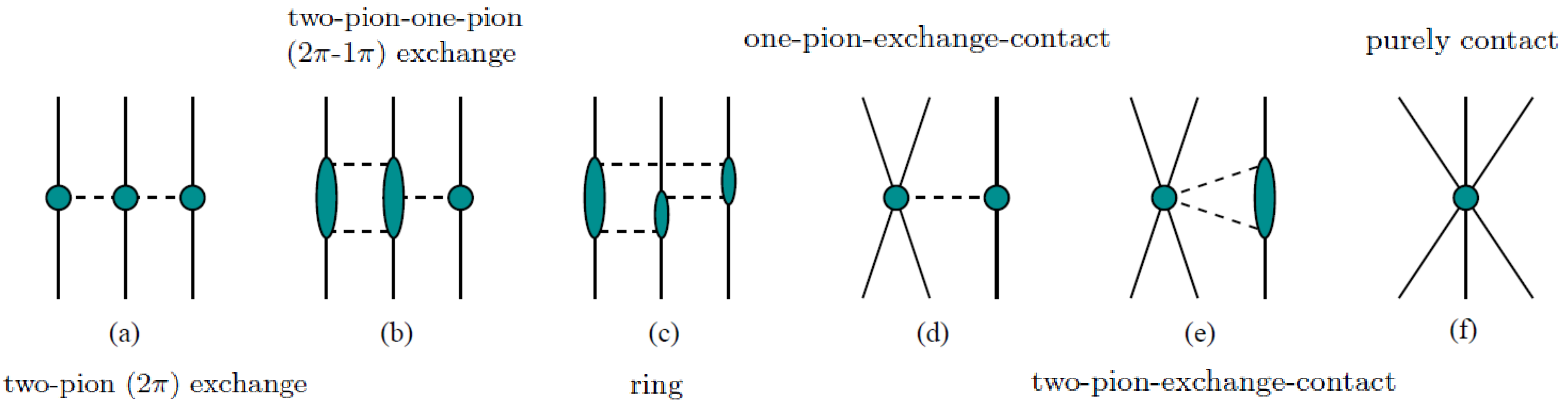


- N$^2$LO: (a) + (d) + (f) (E.Epelbaum et al., PR C66, 064001 (2002))

- N$^3$LO: (a) + (b) + (c) + (d) + (e) + (f) + rel
  V.Bernard et al., PR C77, 064004 (2008) - long range contributions (a), (b), (c)
  V.Bernard et al., PR C84, 054001 (2011) - short range terms (e)
  and leading relativistic corrections

**N$^3$LO contributions do not involve any unknown low energy constants !**

The full N$^3$LO 3NF depends on two parameters D and E coming with (d) and (f) terms, respectively. They are adjusted to two chosen 3N observables.

- N$^4$LO (longest range contributions): (a) + (b) + (c) + (d) + (e) + (f) (H.Krebs et al., arXiv:1203.0067)

**New, efficient method of partial wave expansion:** R.Skibiński et al., PR C84, 054005 (2011)

# 3N basis states

jI-coupling (used during $^3$H and scattering states calculations)

$$\left\langle p'q'(l's')j'(\lambda'\frac{1}{2})I'(j'I')J'M_{J'}\left|V^{3N}\right|pq(ls)j(\lambda\frac{1}{2})I(jI)JM_J\right\rangle$$

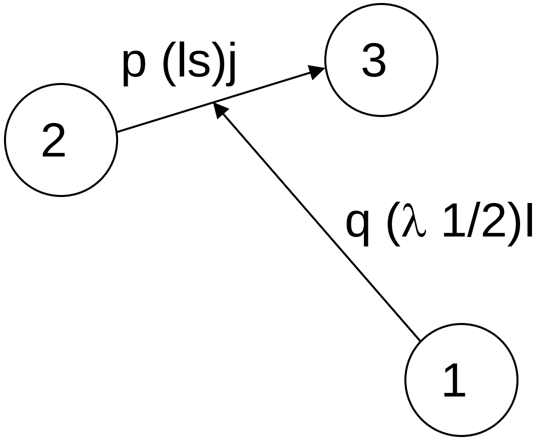


$$\vec{p}=\frac{1}{2}\left(\vec{p}_2-\vec{p}_3\right)$$

$$\vec{q}=\frac{1}{3}\left(2\vec{p}_1-\vec{p}_2-\vec{p}_3\right)$$

LS-coupling (more convenient due to the form of 3NF)

$$\left\langle p'q'(l'\lambda')L'(s'\frac{1}{2})S'(L'S')J'M_{J'}\left|V^{3N}\right|pq(l\lambda)L(s\frac{1}{2})S(LS)JM_J\right\rangle$$

## aPWD of 3NF

$$M \equiv \left\langle p' q' (l' \lambda') L' (s' \frac{1}{2}) S' (L' S') J M_J \left| \hat{O} \right| p q (l \lambda) L (s \frac{1}{2}) S (LS) J M_J \right\rangle =$$

$$= \int d\hat{p} \int d\hat{q} \int d\hat{p}' \int d\hat{q}' \sum_{m_{L'}=-L'}^{L'} c(L', S', J, m_{L'}, M_J - m_{L'}, M_J)$$

$$\sum_{m_L=-L}^{L} c(L, S, J, m_L, M_J - m_L, M_J) \sum_{m_{l'}=-l'}^{l'} c(l', \lambda', L', m_{l'}, m_{L'} - m_{l'}, m_{L'})$$

$$\sum_{m_l=-l}^{l} c(l, \lambda, L, m_l, m_L - m_l, m_L) Y_{l m_l}(\hat{p}) Y^*_{l' m_{l'}}(\hat{p}') Y_{\lambda m_L - m_l}(\hat{q}) Y^*_{\lambda' m_{L'} - m_{l'}}(\hat{q}')$$

$$\left\langle (s' \frac{1}{2}) S' \, M_J - m_{L'} \left| \hat{O}(\vec{p}', \vec{q}', \vec{p}, \vec{q}) \right| (s \frac{1}{2}) S \, M_J - m_L \right\rangle$$

In aPWD one needs to perform:

- 8-dimensional integration for each p',q',p,q
- calculation of the spin-space (isospin-space) element

$$\left\langle (s' \frac{1}{2}) S' \, M_J - m_{L'} \left| \hat{O}(\vec{p}', \vec{q}', \vec{p}, \vec{q}) \right| (s \frac{1}{2}) S \, M_J - m_L \right\rangle$$

**Traditional PWD**:

**Decouple** momentum and spin spaces, **use** properties of the spherical harmonics, Clebsh-Gordan coefficients, 6j and 9j symbols to reduce the number of integrations, **program** (summations, integrals)

# aPWD of 3NF

$$M \equiv \left\langle p'q'(l'\lambda')L'(s'\frac{1}{2})S'(L'S')JM_J \left| \hat{O} \right| pq(l\lambda)L(s\frac{1}{2})S(LS)JM_J \right\rangle =$$

$$= \frac{1}{2J+1} \sum_{M_J=-J}^{J} \left\langle p'q'(l'\lambda')L'(s'\frac{1}{2})S'(L'S')JM_J \left| \hat{O} \right| pq(l\lambda)L(s\frac{1}{2})S(LS)JM_J \right\rangle$$

Since *M* is a scalar quantity, taking

$$\hat{p} = (0,0,1),$$
$$\hat{q} = (\sin\theta_q, 0, \cos\theta_q)$$

reduces the number of integrations to 5.
The isospin matrix elements can be easily calculated analyticaly.
The spin matrix elements can be calculated using a software for symbolic algebra (for example *Mathematica*®).

The remainig task is still hard numerically ($10^7$ 5-dim integrations).

details: R.Skibiński et al., PR C84, 054005 (2011)

# Test: aPWD vs PWD for 3NF

Example: 2π-exchange potential for the Tucson-Melbourne 3NF

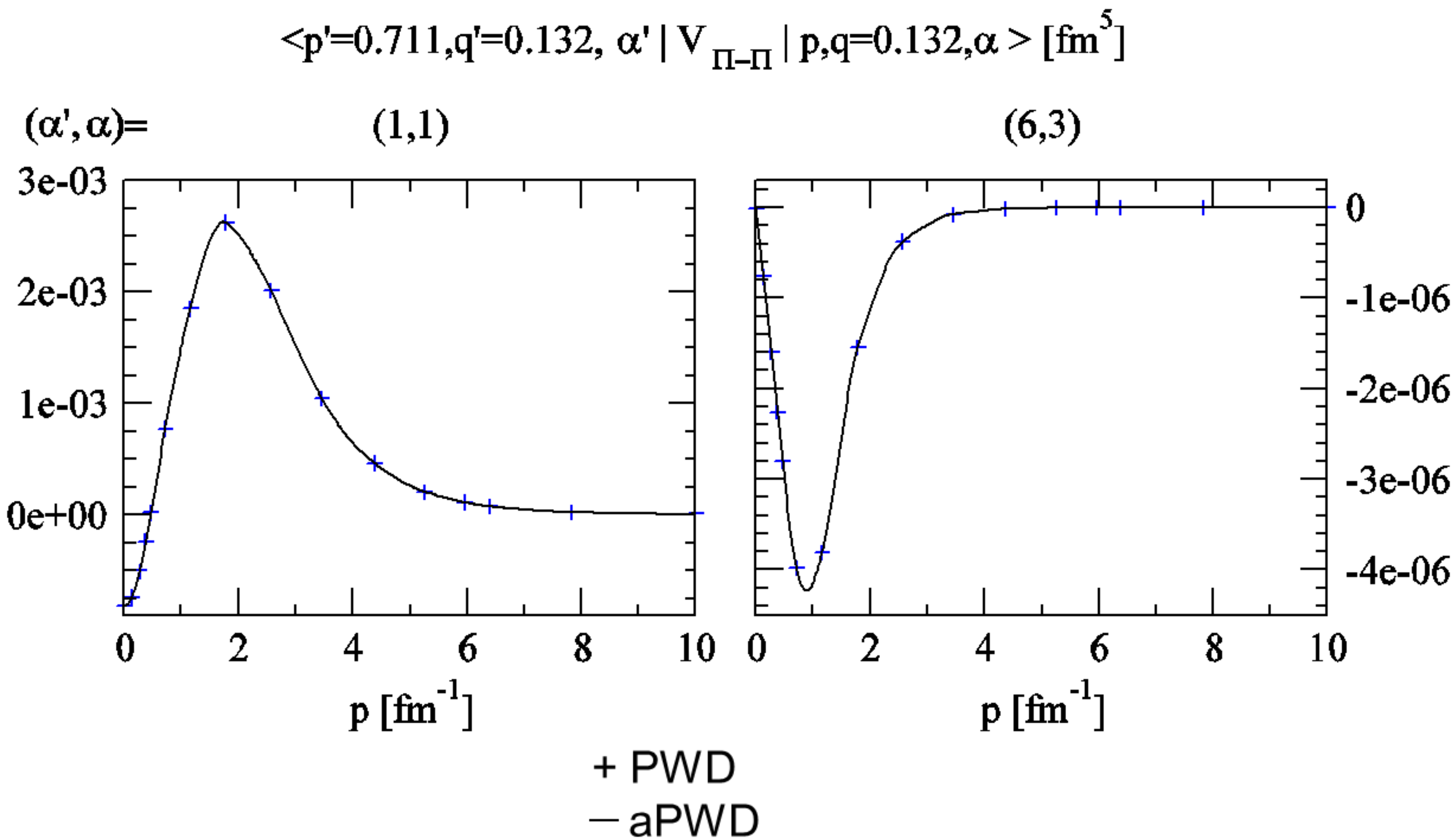

# Values of free parameters d and e

- Values of the d and e constants are obtained from the fit to $^3$H binding energy and $^2a_{nd}$ scattering length. Here only long range terms of 3NF supplemented by d- and e- short range terms are taken into account.

| Cut-off | $\Lambda$ [MeV] | d | e |
|---|---|---|---|
| 1 | 450 | 11.4 | 0.56 |
| 2 | 600 | 12.03 | 2.196 |
| 3 | 550 | 11.85 | 3.04 |
| 4 | 450 | 7.59 | -0.063 |
| 5 | 600 | 14.1 | 2.649 |

$$d = D \cdot F_\pi^2 \cdot \Lambda_\chi$$

$$e = E \cdot F_\pi^4 \cdot \Lambda_\chi$$

$F_\pi$= 92.4 MeV
$\Lambda_\chi$= 700 MeV

- d and e are large compared to their values at N$^2$LO:
- e.g cut-off=3: d=-0.45 e=-0.798 but
- $^2a_{nd}$ : exp: 0.645 fm, for pure NN: N$^2$LO: 0.794 fm, N$^3$LO:1.5873 fm.

# $^3$H at N$^3$LO with relativistic corrections to 3NF (cut-off=1)

- New values of d and e

| | d | e |
|---|---|---|
| $V_{\pi\pi}+V_{2\pi-1\pi}+V_{ring}+V_d+V_e$ | **11.4** | **0.56** |
| $V_{\pi\pi}+V_{2\pi-1\pi}+V_{ring}+V_d+V_e+V_{2\pi\text{-cont}}$ | **13.442** | **0.206** |
| $V_{\pi\pi}+V_{2\pi-1\pi}+V_{ring}+V_d+V_e+V_{2\pi\text{-cont}}+V_{1/m}$ | **13.78** | **0.372** |

- Expectation values [MeV]

| | $E_{NN}$ | $E_{3NF}$ |
|---|---|---|
| $V_{\pi\pi}+V_{2\pi-1\pi}+V_{ring}+V_d+V_e$ | **-43.449** | **-0.996** |
| $V_{\pi\pi}+V_{2\pi-1\pi}+V_{ring}+V_d+V_e+V_{2\pi\text{-cont}}$ | **-43.399** | **-1.024** |
| $V_{\pi\pi}+V_{2\pi-1\pi}+V_{ring}+V_d+V_e+V_{2\pi\text{-cont}}+V_{1/m}$ | **-43.382** | **-1.017** |

| | $V_{\pi\pi}$ | $V_{2\pi-1\pi}$ | $V_{ring}$ | $V_{2\pi\text{-cont}}$ | $V_{d\text{-term}}$ | $V_{e\text{-term}}$ | $V_{1/m}$ |
|---|---|---|---|---|---|---|---|
| $V_{\pi\pi}+V_{2\pi-1\pi}+V_{ring}+V_d+V_e$ | **-0.648** | **0.470** | **0.015** | **---------** | **-0.746** | **-0.087** | **--------** |
| $V_{\pi\pi}+V_{2\pi-1\pi}+V_{ring}+V_d+V_e+V_{2\pi\text{-cont}}$ | **-0.661** | **0.485** | **0.014** | **0.082** | **-0.912** | **-0.032** | **--------** |
| $V_{\pi\pi}+V_{2\pi-1\pi}+V_{ring}+V_d+V_e+V_{2\pi\text{-cont}}+V_{1/m}$ | **-0.655 (100%)** | **0.481 (73.4%)** | **0.014 (2.1%)** | **0.082 (12.5%)** | **-0.930 (142%)** | **-0.057 (8.7%)** | **0.048 (7.3%)** |

# $A_y$ puzzle

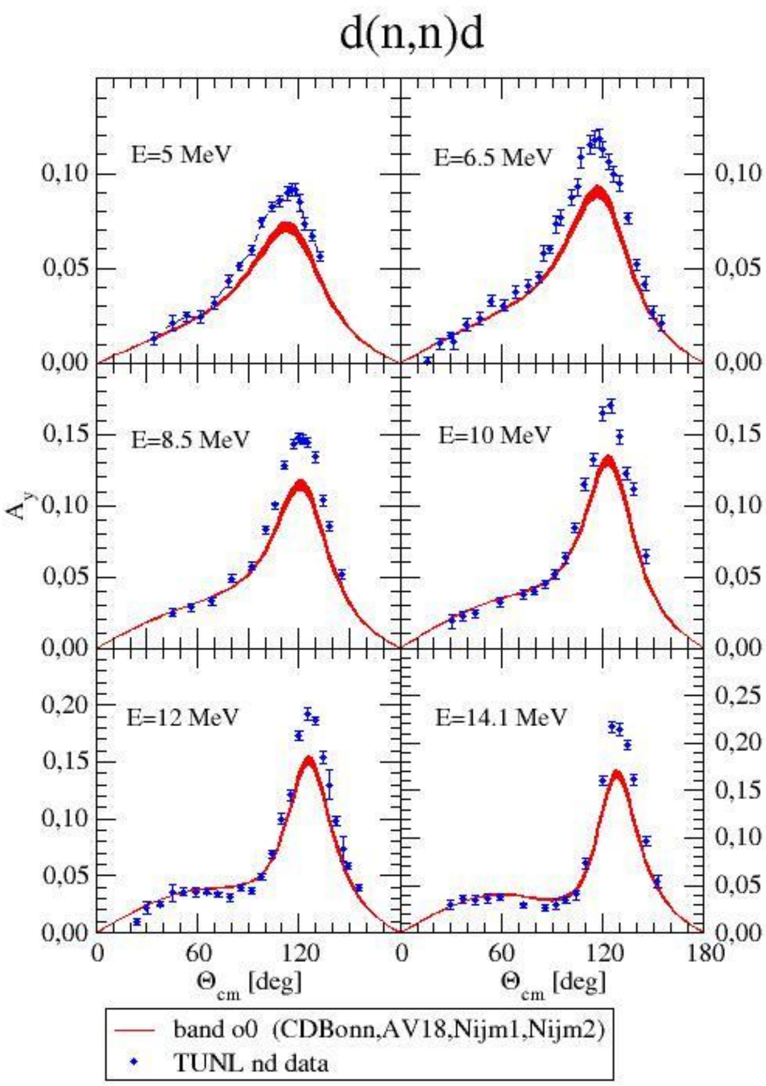


**Sensitivity to $^3P_j$ NN force components:**

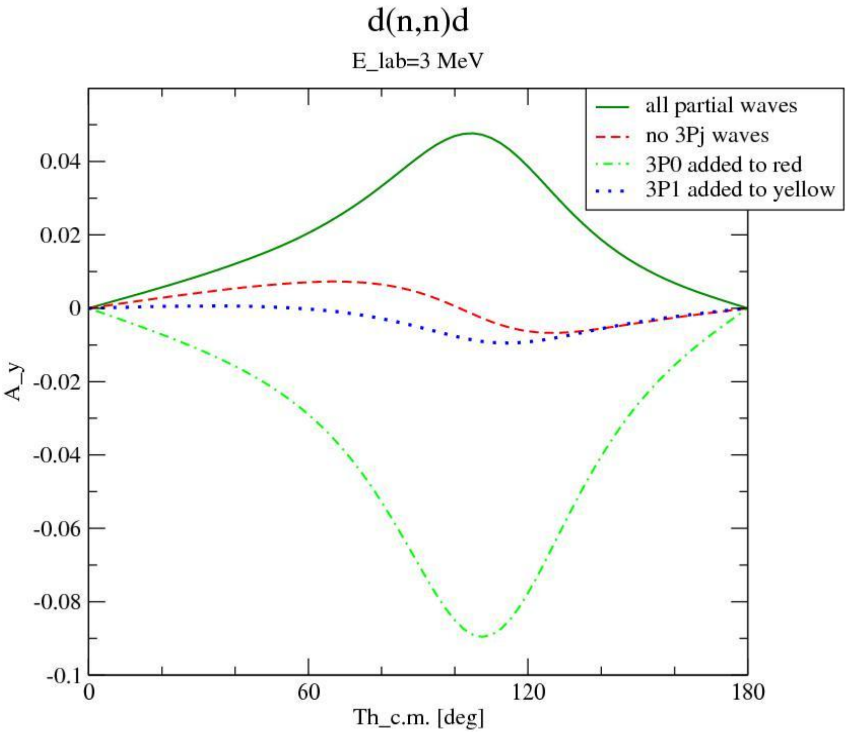

# $A_y$ puzzle

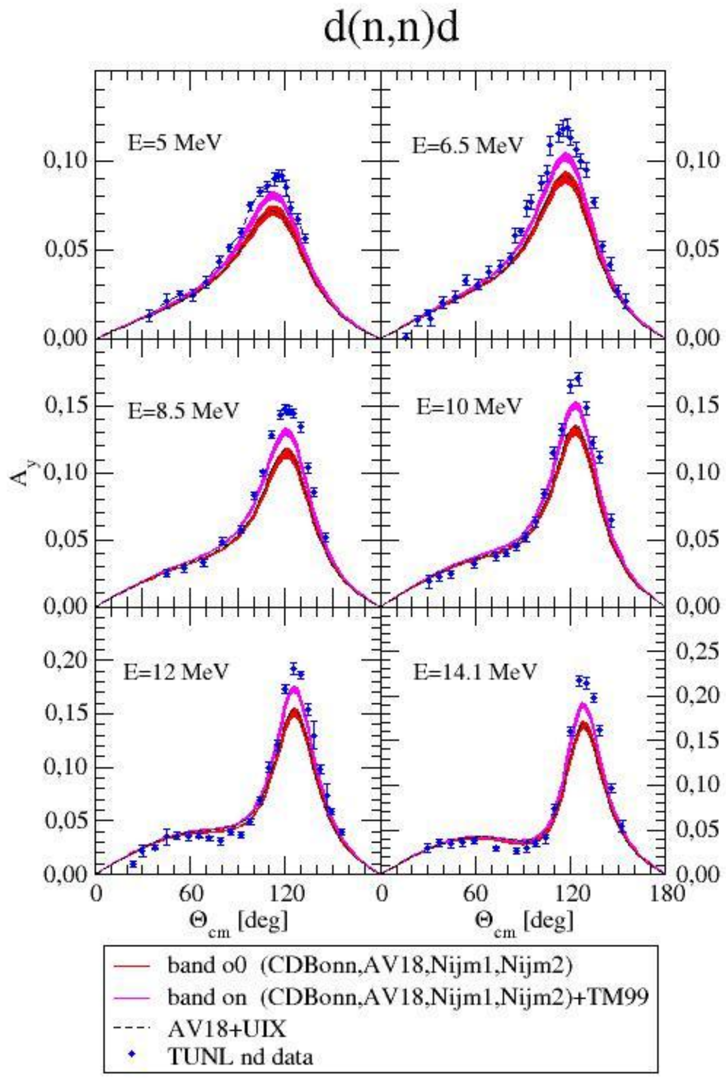

d(n,n)d
E=5 MeV
E=6.5 MeV
E=8.5 MeV
E=10 MeV
E=12 MeV
E=14.1 MeV
A_y
Θ_cm [deg]
Θ_cm [deg]
band o0 (CDBonn,AV18,Nijm1,Nijm2)
band on (CDBonn,AV18,Nijm1,Nijm2)+TM99
AV18+UIX
TUNL nd data

# $A_y$ puzzle

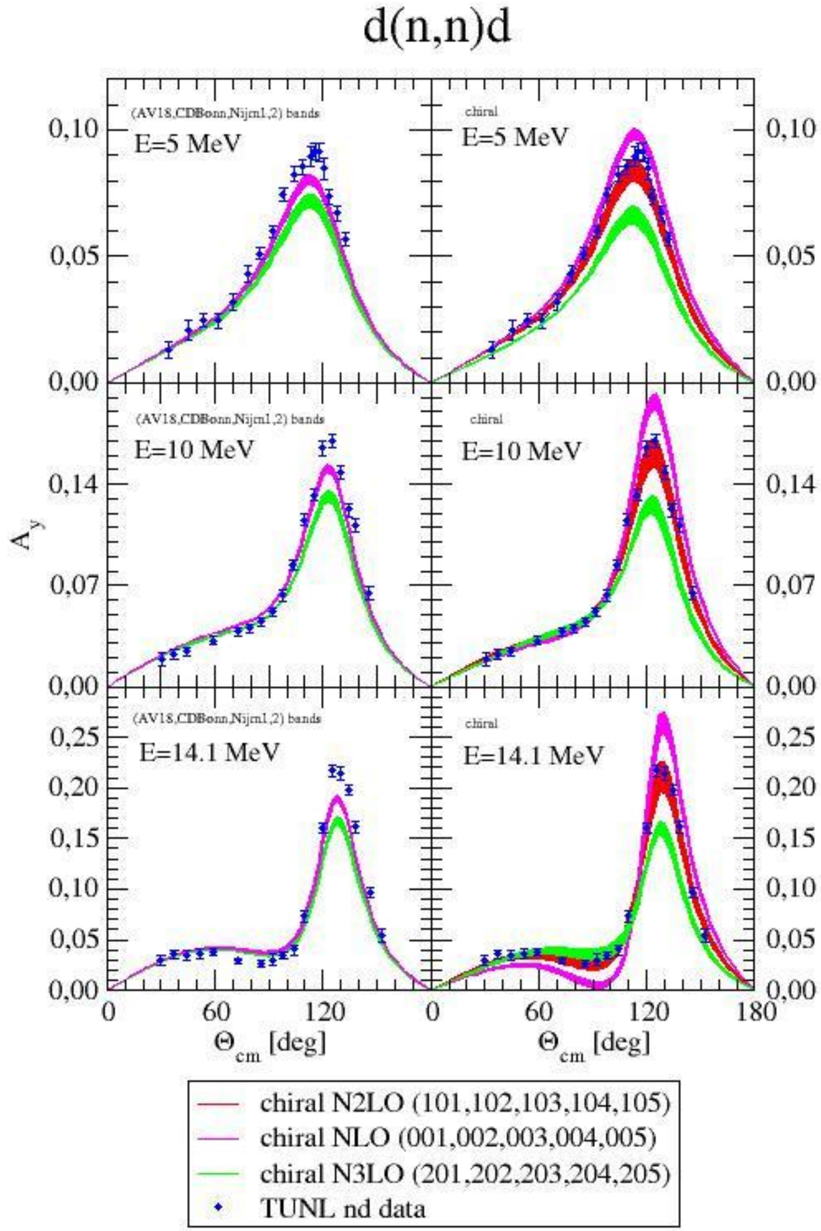

d(n,n)d
(AV18,CDBonn,Nijm1,2) bands
chiral
E=5 MeV
E=10 MeV
E=14.1 MeV
$A_y$
$\Theta_{cm}$ [deg]
chiral N2LO (101,102,103,104,105)
chiral NLO (001,002,003,004,005)
chiral N3LO (201,202,203,204,205)
TUNL nd data


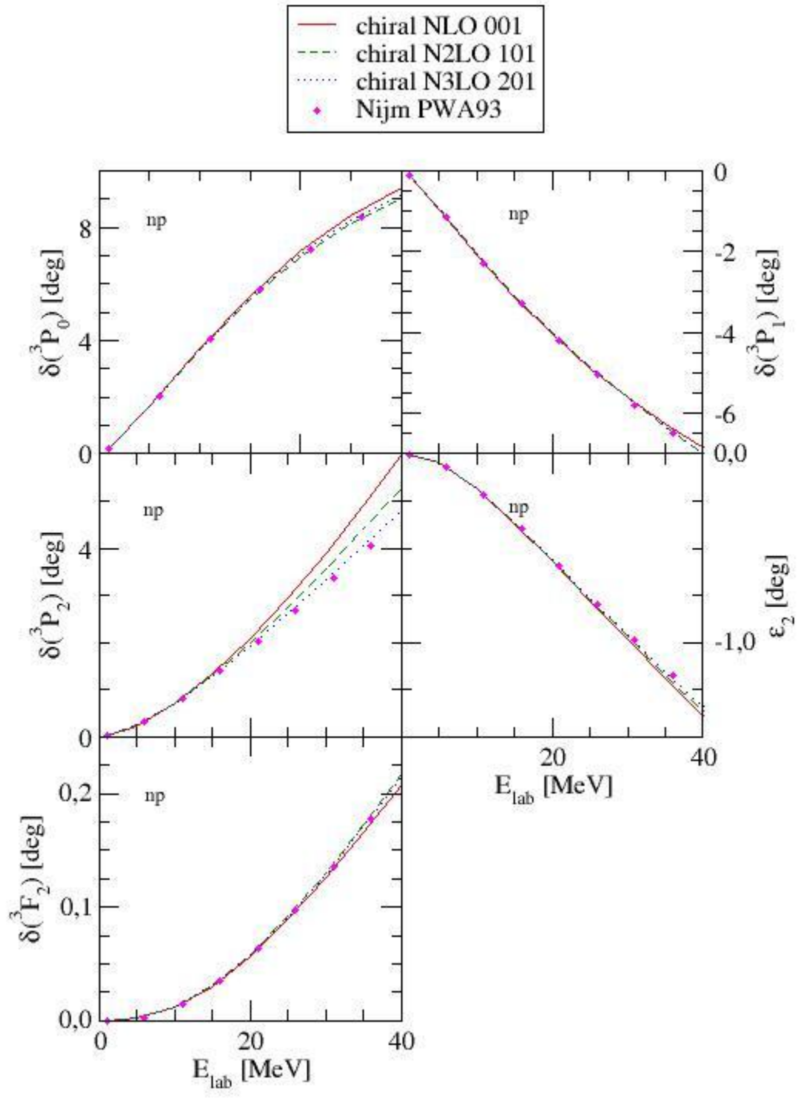

chiral NLO 001
chiral N2LO 101
chiral N3LO 201
Nijm PWA93
np
$\delta(^3P_0)$ [deg]
$\delta(^3P_1)$ [deg]
$\delta(^3P_2)$ [deg]
$\varepsilon_2$ [deg]
$\delta(^3F_2)$ [deg]
$E_{lab}$ [MeV]

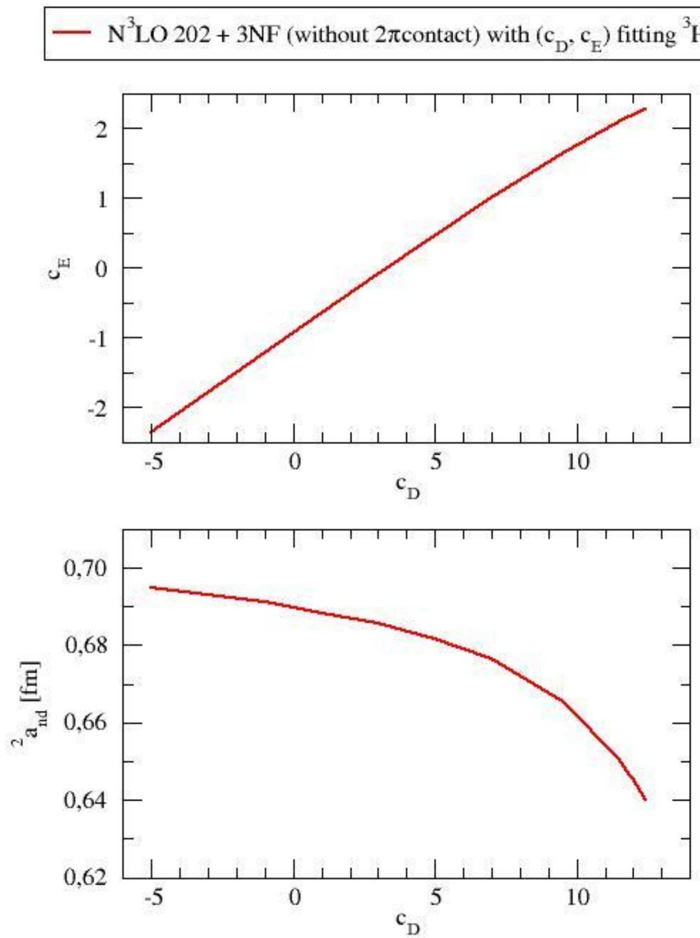

N3LO 202 + 3NF (without 2πcontact) with (cD, cE) fitting 3H
cE
cD
2a nd [fm]
cD


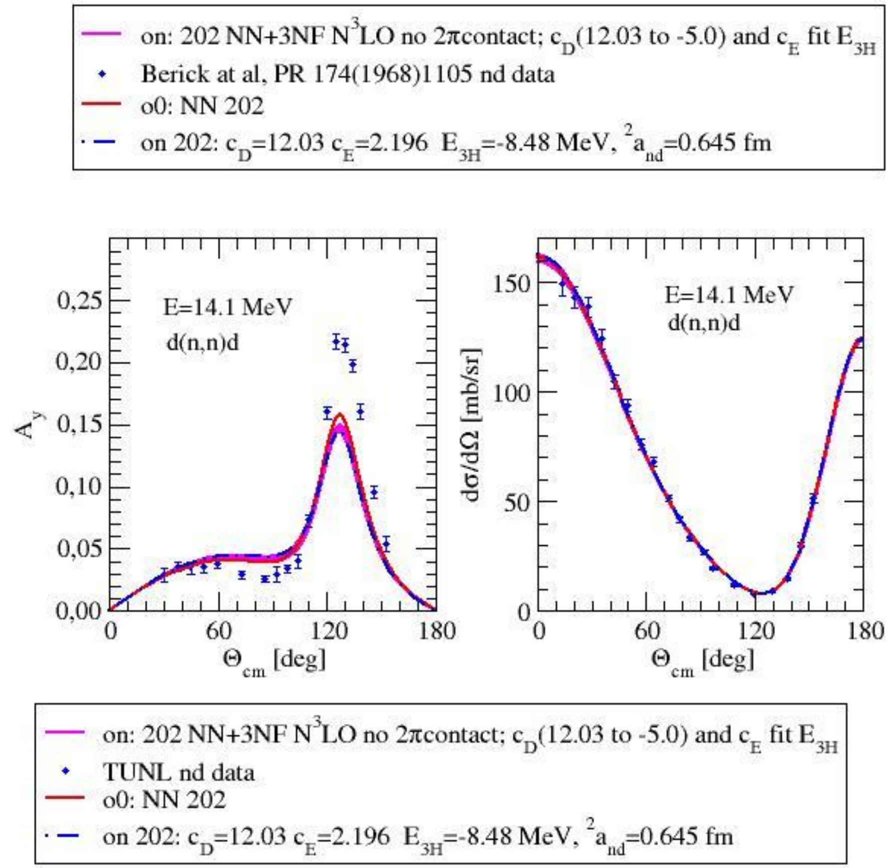

on: 202 NN+3NF N3LO no 2πcontact; cD(12.03 to -5.0) and cE fit E3H
Berick at al, PR 174(1968)1105 nd data
o0: NN 202
on 202: cD=12.03 cE=2.196 E3H=-8.48 MeV, 2and=0.645 fm
E=14.1 MeV
d(n,n)d
Ay
Θcm [deg]
E=14.1 MeV
d(n,n)d
dσ/dΩ [mb/sr]
Θcm [deg]
on: 202 NN+3NF N3LO no 2πcontact; cD(12.03 to -5.0) and cE fit E3H
TUNL nd data
o0: NN 202
on 202: cD=12.03 cE=2.196 E3H=-8.48 MeV, 2and=0.645 fm

# $A_y$ puzzle: $N^3LO$ 3NF with short-ranged $2\pi$-contact term

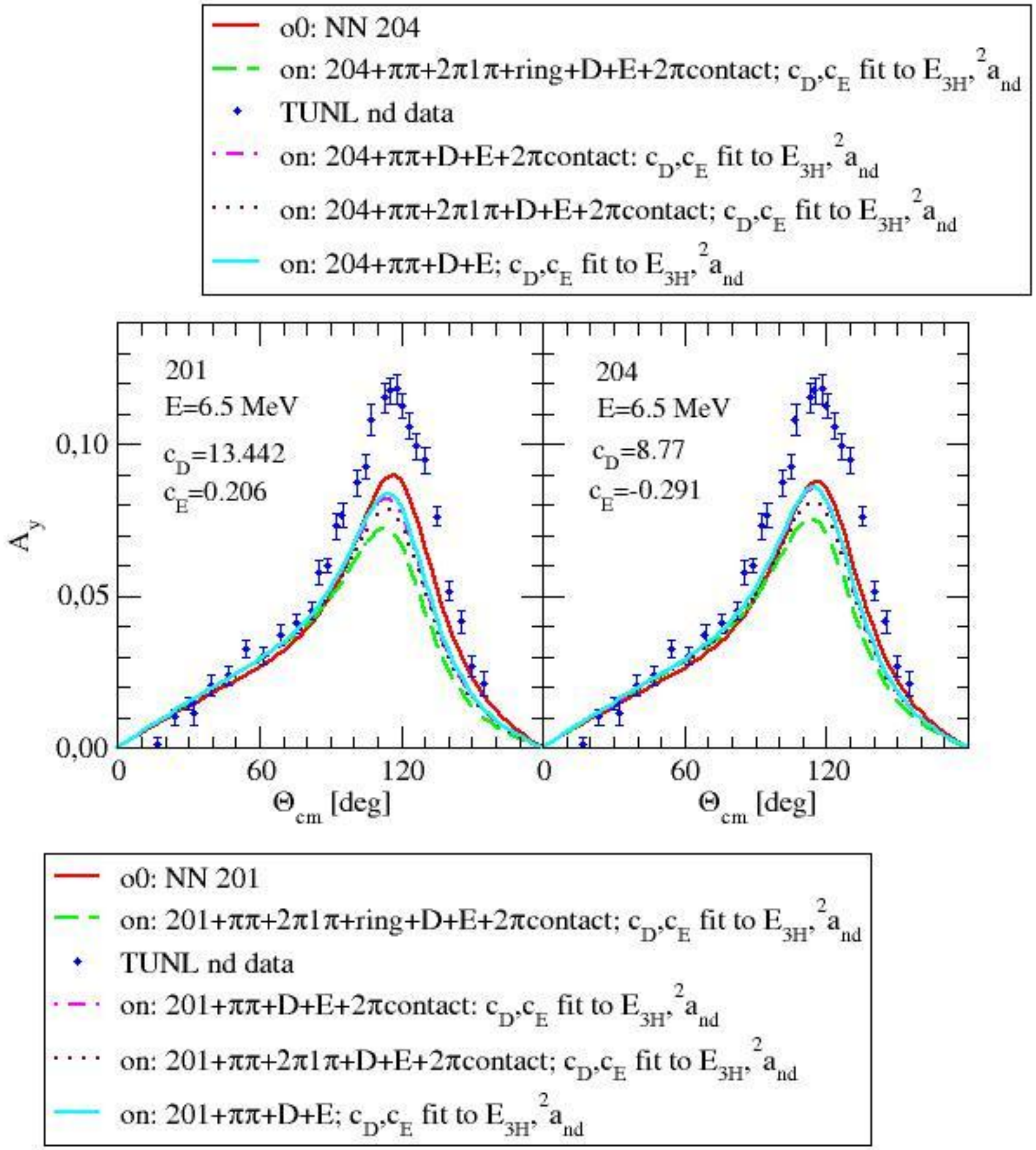

## Conclusions:

- at low energies effects of $N^3LO$ 3NF's are rather small
- they do not decrease the discrepancy between data and theory in the maximum of $A_y$
- it indicates that probably $A_y$ puzzle reflects bad knowledge of low energy $^3P_j$ NN forces

# Breakup symmetric-space-star (SST) configuration:

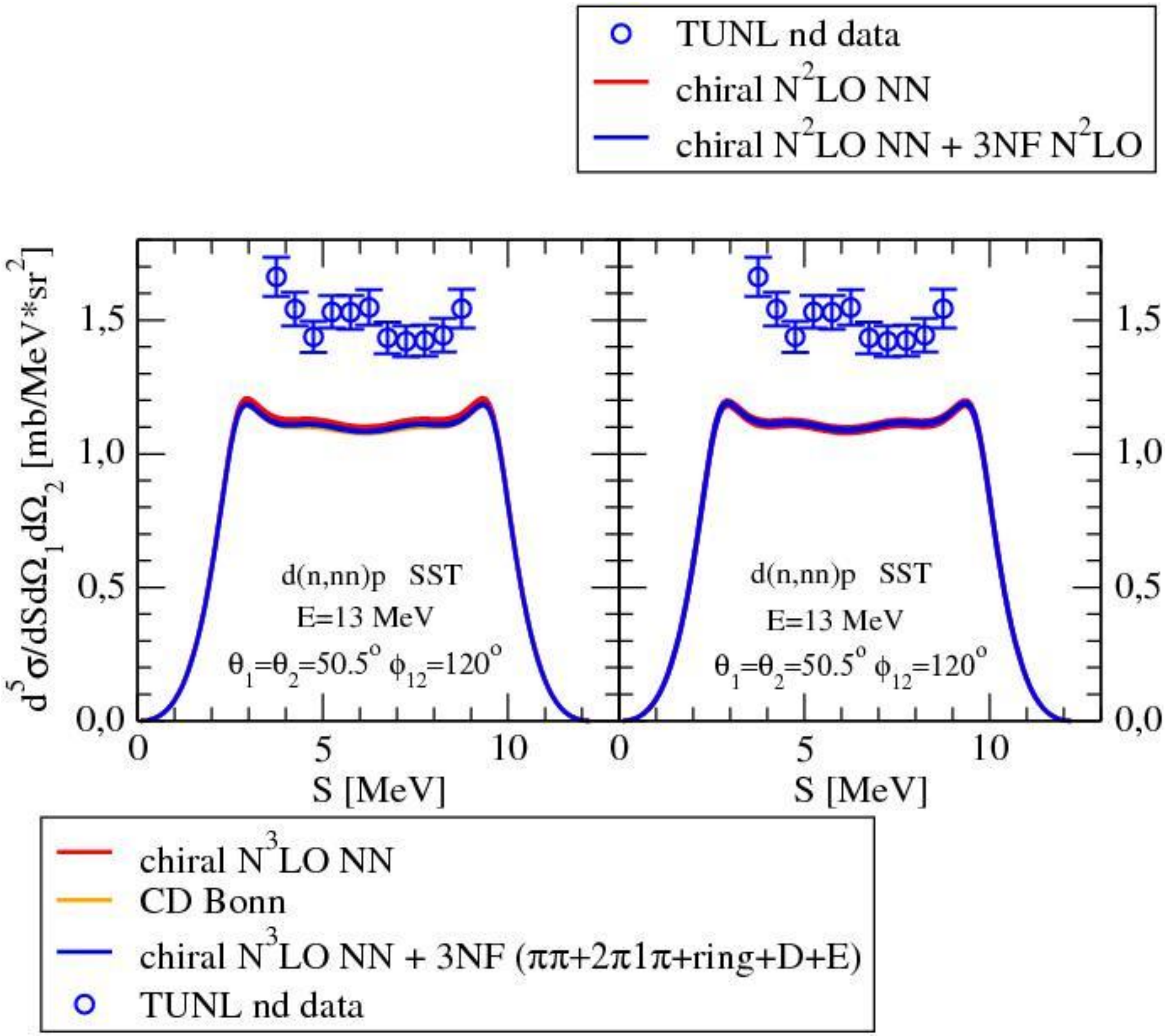

# Breakup quasi-free-scattering (QFS) configuration:

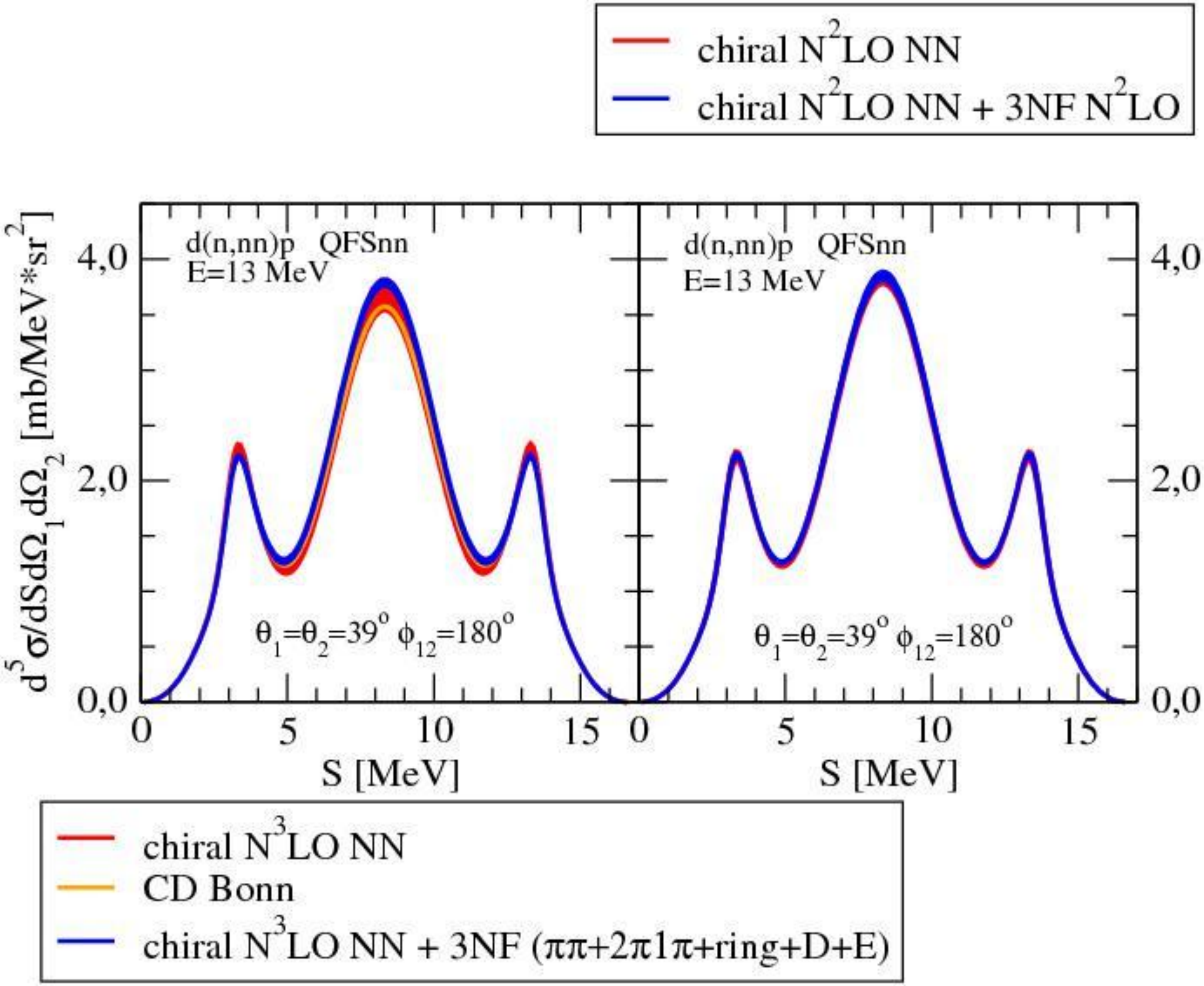

# Contributions of $^1S_0$, $^3S_1$ and other partial waves:

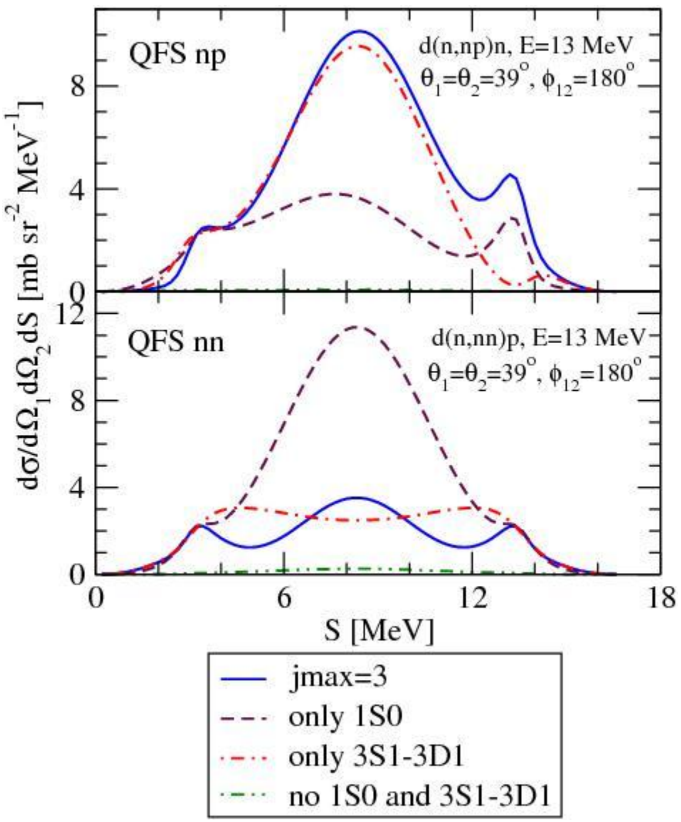


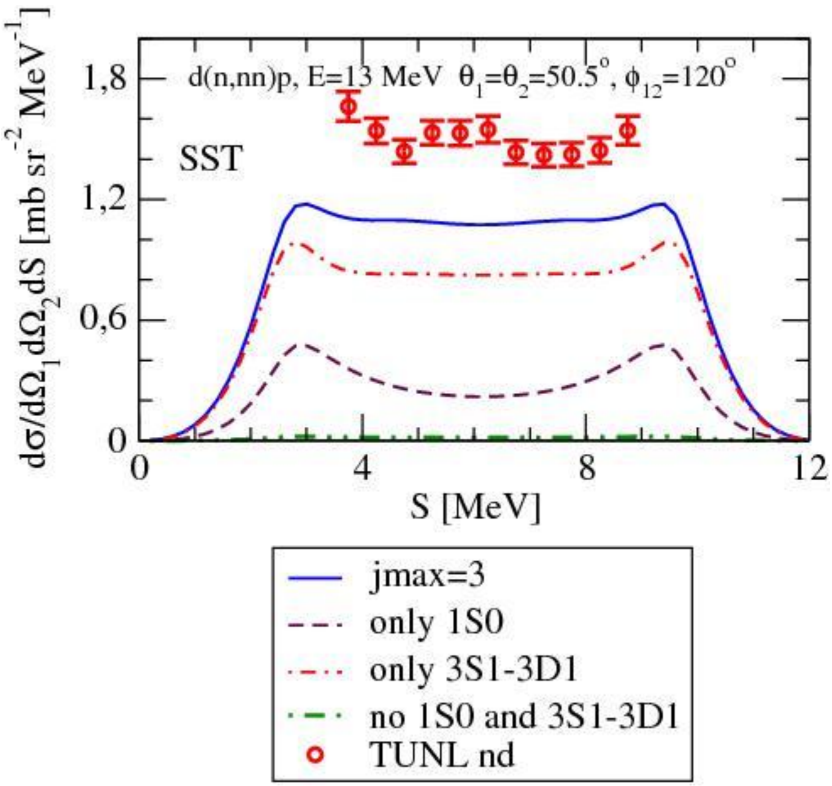

- For low-energy free np and nn scatterings one expects the largest contribution from S-waves
- For np it will be $^3S_1 - {}^3D_1$ and $^1S_0$ np interaction
- For nn it will be $^1S_0$ nn force (nn cannot interact through $^3S_1 - {}^3D_1$)
- Therefore: **free np scattering is sensitive to $^3S_1 - {}^3D_1$ and $^1S_0$ np forces**
  **free nn scattering is sensitive to $^1S_0$ nn force**

- Simple minded picture of QFS is that one of the three nucleons (at rest in lab. system) is just a spectator
- Thus QFS should be practically insensitive to the action of 3NF and, if higher order rescatterings will not distroy that simple picture, the above dominance should be present

- That means **that the nn QFS would be a powerfull tool to study the $^1S_0$ nn force component**
- np (and pp) forces are rather good nailed down by 2N scattering data (PWA)
- Therefore **one should not expect surprises for np QFS (and pp QFS) data**
- Such **surprises can be expected for nn QFS data** (no nn 2N data)

QFSnp: d(n,np)n, En=26 MeV

$\Theta_n = 39°$ $\Theta_p = 42°$ $\phi_{np} = 180°$

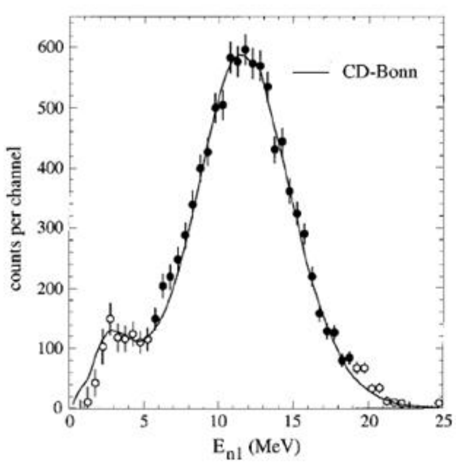


FIG. 2. Data for $n$-$p$ QFS, projected onto the $E_n$ axis. The solid line is the finite-geometry Monte Carlo prediction, using CD-Bonn for the $N$-$N$ interaction.

QFSnn: d(n,nn)p, En=26 MeV

Both $n$ detectors were at $\Theta_n = 42°$

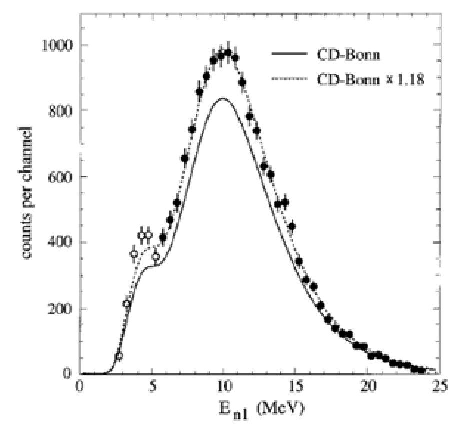


FIG. 4. HE data of Fig. 3, projected onto the $E_{n1}$ axis. The solid curve represents the finite-geometry Monte Carlo prediction using CD-Bonn, the dotted line is the MC result normalized to the experiment by multiplication with a factor of 1.18. Only events with $E_{n1}$ and $E_{n2} > 6$ MeV have been included in the analysis.

PR C65, 034010 (2002)

## Insensitivity of QFS configuration to underlying dynamics:

**shown with different (practically overlapping lines) are results based on CD Bonn, Nijm I, Nijm II and their combinations with TM99 3NF**

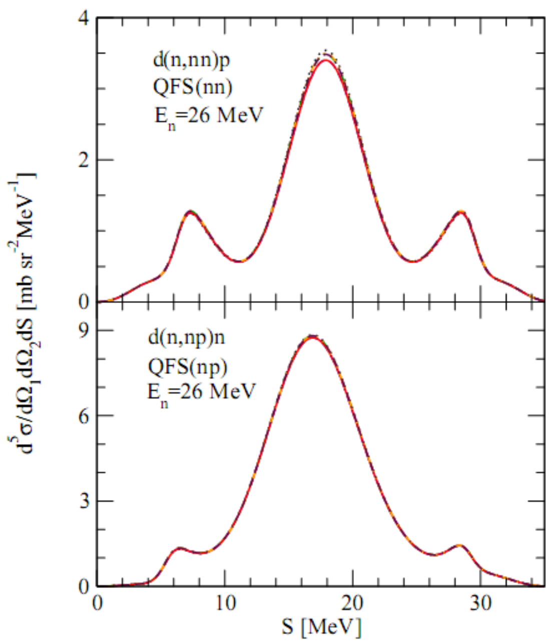


FIG. 1: (color online) The cross section $d^5\sigma/d\Omega_1 d\Omega_2 dS$ for the $E_n^{lab} = 26$ MeV nd breakup reaction $d(n,nn)p$ (upper panel) and $d(n,np)n$ (lower panel) as a function of the S-curve length for two complete configurations of Ref. [4]. QFS nn refers to the angles of the two neutrons: $\theta_1 = \theta_2 = 42^o$ and QFS np refers to the angle $\theta_1 = 39^o$ of the detected neutron and $\theta_2 = 42^o$ for the proton. In both cases $\phi_{12} = 180^o$. The (practically overlapping) lines correspond to different underlying dynamics: CD Bonn [8] - dashed (blue), Nijm I - dotted (black), Nijm II [9] - dashed-dotted (green), CD Bonn+TM99 - solid (red), Nijm I +TM99 [10, 11] - dashed-double-dotted (orange), Nijm II + TM99 - double-dashed-dotted (maroon). All partial waves with 2N total angular momenta up to $j_{max} = 5$ have been included.

## Contributions from different NN force components:

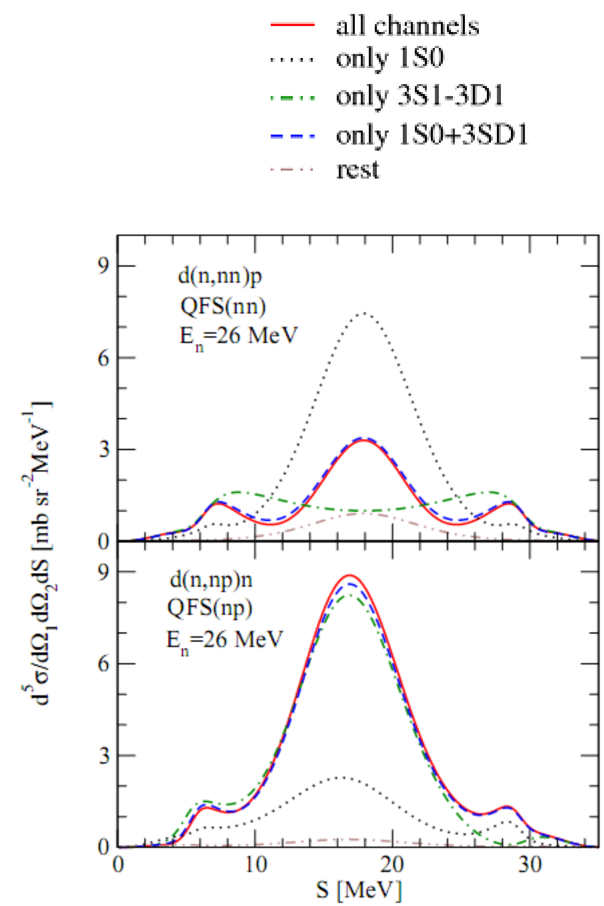


FIG. 2: (color online) The cross section $d^5\sigma/d\Omega_1 d\Omega_2 dS$ for the $E_n^{lab} = 26$ MeV nd breakup reaction $d(n,nn)p$ (upper panel) and $d(n,np)n$ (lower panel) as a function of the S-curve length for two complete configurations of Ref. [4] specified in Fig. 1. The different lines show contributions from different NN force components. The solid (red) line is the full result based on the CD Bonn potential [8] and all partial waves with 2N total angular momenta up to $j_{max} = 5$ included. The dotted (black), dashed-dotted (green), and dashed (blue) lines result when only contributions from ${}^1S_0$, ${}^3S_1 - {}^3D_1$, and ${}^1S_0 + {}^3S_1 - {}^3D_1$ are kept calculating the cross sections. The dashed-double-dotted (brown) line presents the contribution of all partial waves with the exception of ${}^1S_0$ and ${}^3S_1 - {}^3D_1$.

# Sensitivity of QFS nn to changes in the nn $^1S_0$ force component:

$$V_{nn}(^1S_0) = \lambda * V_{CD\ Bonn}(^1S_0)$$

| $\lambda$ | $\epsilon_{nn}$ [MeV] | $a_{nn}$ [fm] | $r_{eff}$ [fm] |
|---|---|---|---|
| 0.9 | - | -8.25 | 3.12 |
| 1.0 | - | -18.80 | 2.82 |
| 1.19 | -0.099 | +21.69 | 2.39 |
| 1.21 | -0.144 | +18.22 | 2.35 |
| 1.3 | -0.441 | +10.95 | 2.20 |
| 1.4 | -0.939 | +7.87 | 2.07 |

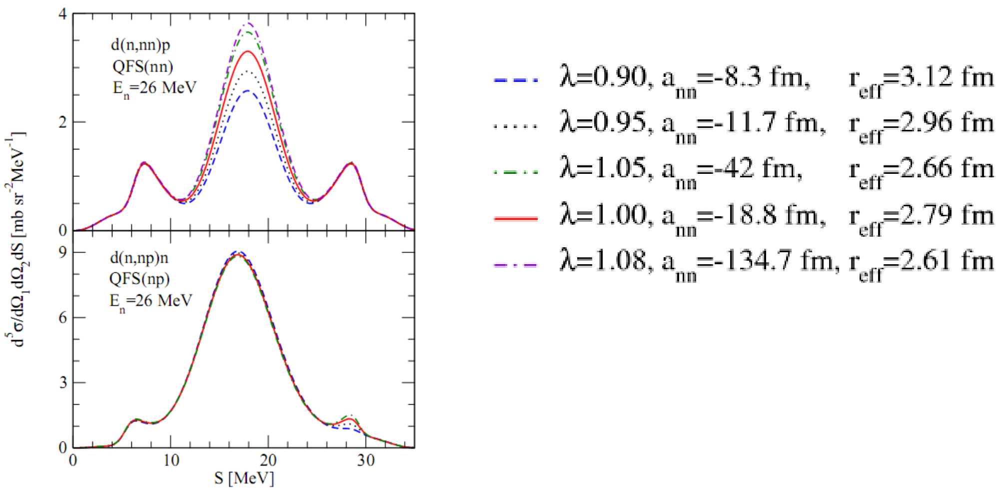


FIG. 3: (color online) The cross section $d^5\sigma/d\Omega_1 d\Omega_2 dS$ for the $E_n^{lab} = 26$ MeV nd breakup reaction $d(n,nn)p$ (upper panel) and $d(n,np)n$ (lower panel) as a function of the S-curve length for two complete configurations of Ref. [4] specified in Fig. 1. The lines show sensitivity of the QFS cross sections to the changes of the nn $^1S_0$ force component. Those changes were induced by multiplying the $^1S_0$ nn matrix element of the CD Bonn potential by a factor $\lambda$. The solid (red) line is the full result based on the original CD Bonn potential [8] ($a_{nn} = -18.8$ fm, $r_{eff} = 2.79$ fm) and all partial waves with 2N total angular momenta up to $j_{max} = 5$ included. The dashed (blue), dotted (black), and dashed-dotted (green) lines correspond to $\lambda = 0.9$ ($a_{nn} = -8.3$ fm, $r_{eff} = 3.12$ fm), 0.95 ($a_{nn} = -11.7$ fm, $r_{eff} = 2.96$ fm), and 1.05 ($a_{nn} = -42.0$ fm, $r_{eff} = 2.66$ fm), respectively. The double-dashed-dotted (violet) line shows cross sections obtained with $\lambda = 1.08$ ($a_{nn} = -134.7$ fm, $r_{eff} = 2.61$ fm), which factor is required to get agreement with nn QFS data of ref. [4].

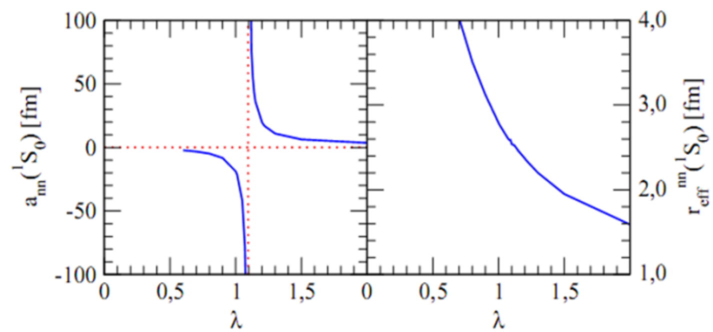


FIG. 4: (color online) The changes of the nn scattering length $a_{nn}$ and the effective range parameter $r_{eff}$ with factor $\lambda$ by which the $^1S_0$ nn matrix element of the CD Bonn potential is multiplied: $V_{nn}(^1S_0) = \lambda * V_{CD\ Bonn}(^1S_0)$.

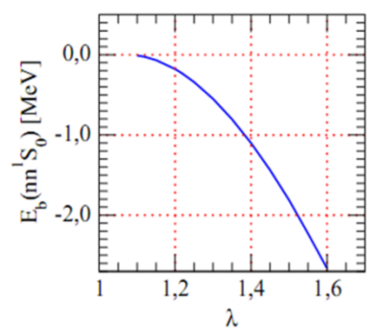


FIG. 5: (color online) The range of $\lambda$ values by which the $^1S_0$ nn matrix element of the CD Bonn potential is multiplied ($V_{nn}(^1S_0) = \lambda * V_{CD\ Bonn}(^1S_0)$), for which the two neutrons form a bound state with the binding energy $E_b$.

- to remove 18% discrepancy found in experiment for nn QFS would require a value of λ ~ 1.08
- such increased strength in the $^1S_0$ nn interaction would drastically decrease $^1S_0$ nn scattering length to ann= -135 fm
- **it would lead to a nearly bound state of two neutrons in $^1S_0$**

# What are consequences of $^{1}S_{0}$ dineutron for description of nd data ?

| $\lambda$ | $\epsilon_{nn}$ [MeV] | $a_{nn}$ [fm] | $r_{eff}$ [fm] |
|---|---|---|---|
| 0.9 | - | -8.25 | 3.12 |
| 1.0 | - | -18.80 | 2.82 |
| 1.19 | -0.099 | +21.69 | 2.39 |
| 1.21 | -0.144 | +18.22 | 2.35 |
| 1.3 | -0.441 | +10.95 | 2.20 |
| 1.4 | -0.939 | +7.87 | 2.07 |

Total nd cross section

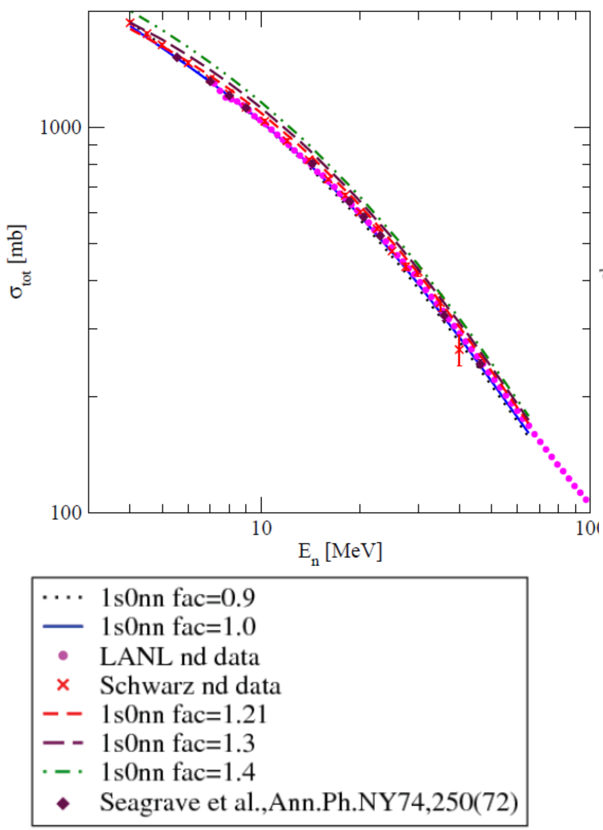


Total nd elastic scattering cross section

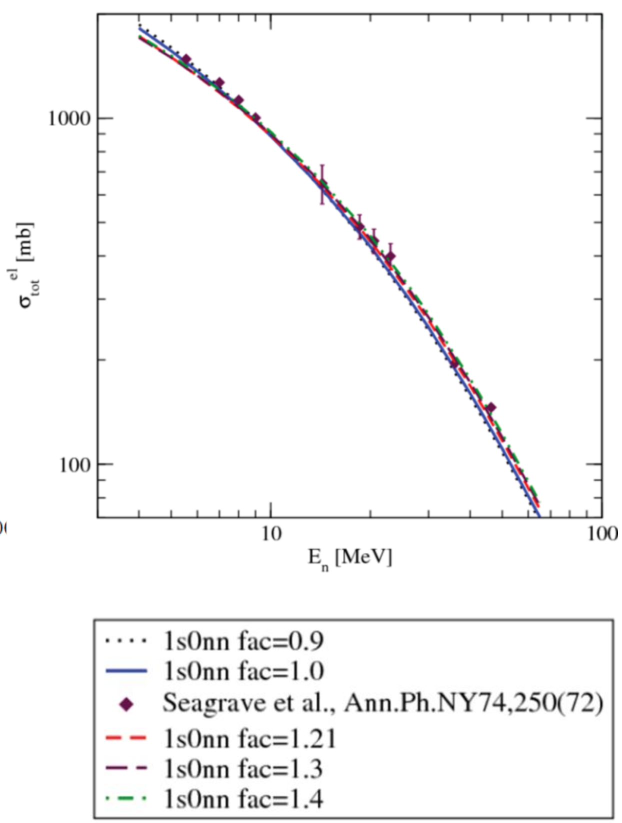


Total nd breakup cross section

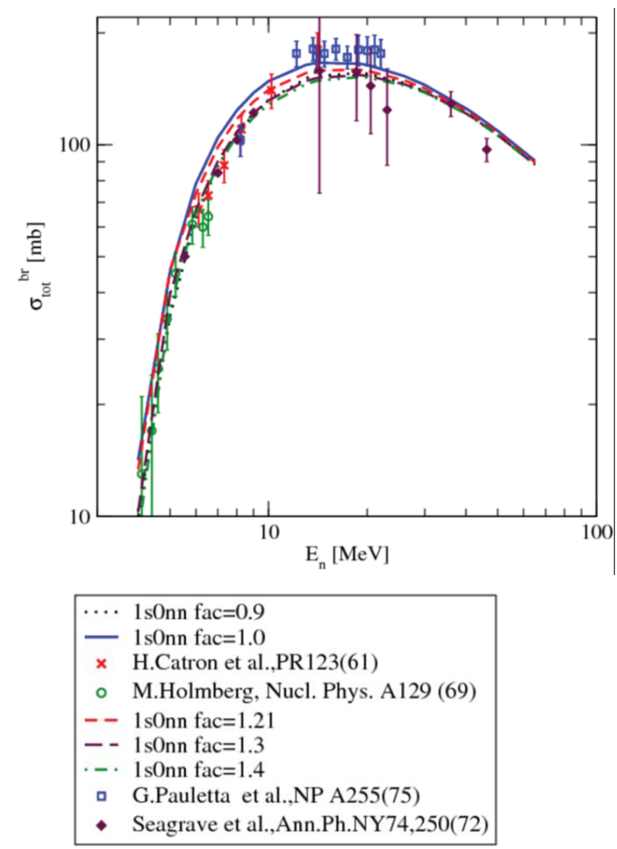

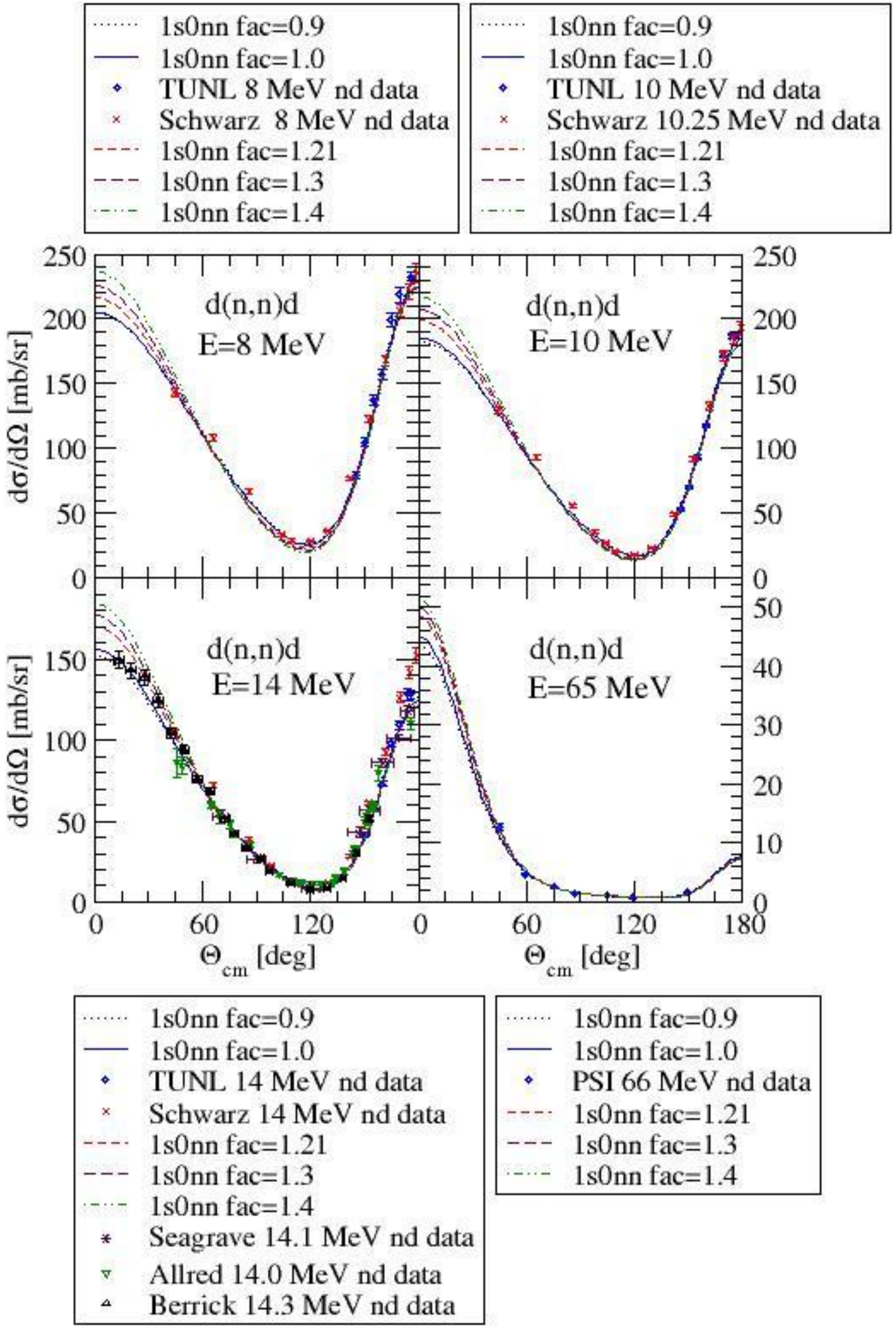


| $\lambda$ | $\epsilon_{nn}$ [MeV] | $a_{nn}$ [fm] | $r_{eff}$ [fm] |
|---|---|---|---|
| 0.9 | - | -8.25 | 3.12 |
| 1.0 | - | -18.80 | 2.82 |
| 1.19 | -0.099 | +21.69 | 2.39 |
| 1.21 | -0.144 | +18.22 | 2.35 |
| 1.3 | -0.441 | +10.95 | 2.20 |
| 1.4 | -0.939 | +7.87 | 2.07 |

**Nd elastic scattering angular distributions:**

**precise forward angle cross section data would be required to test the dineutron existence**

- **The strongest argument against dineutron** is provided by four measured FSI nn configurations (PRC73,034001(2006)).
- Their analyses gave **consistent negative $^1S_0$ $a_{nn}$ values in all four configurations measured**.
- **With positive $a_{nn}$ the extracted values would be configuration-dependent !**

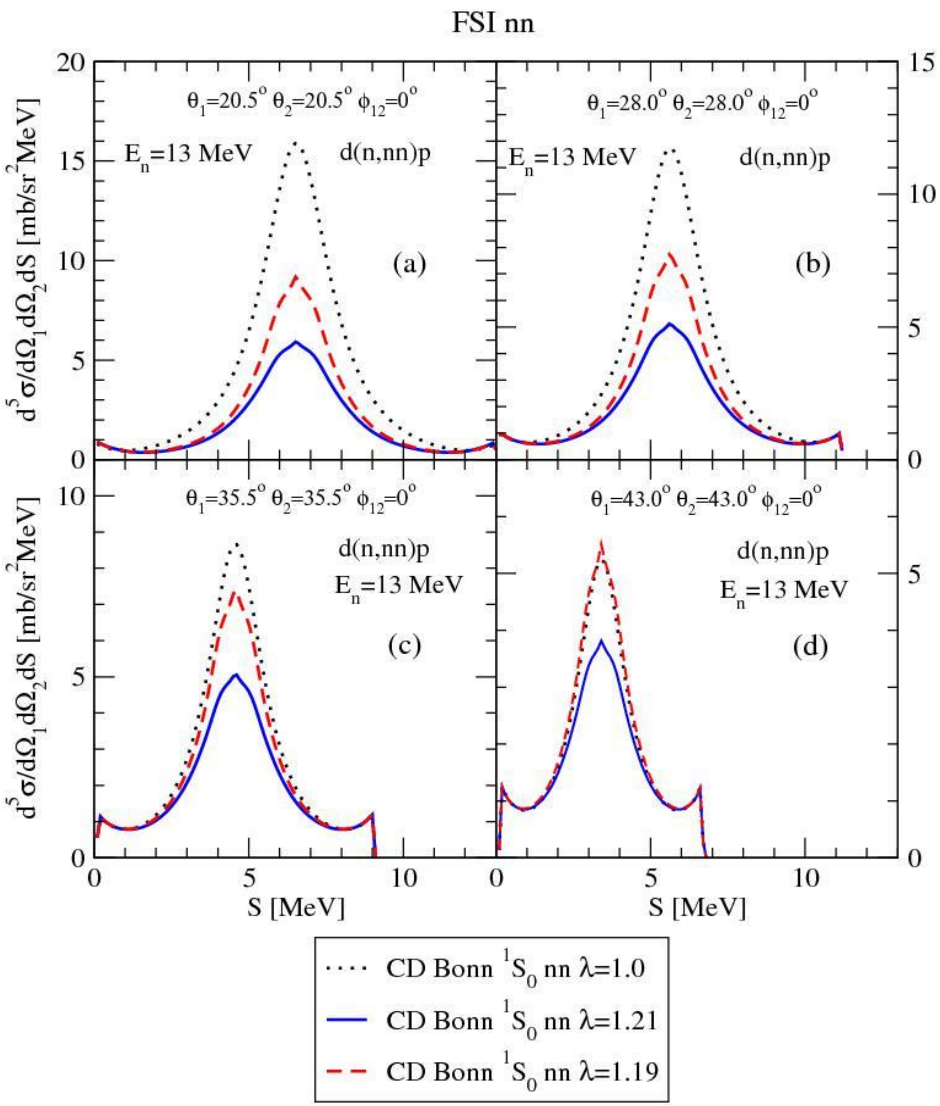


| $\lambda$ | $\epsilon_{nn}$ [MeV] | $a_{nn}$ [fm] | $r_{eff}$ [fm] |
|---|---|---|---|
| 0.9 | - | -8.25 | 3.12 |
| 1.0 | - | -18.80 | 2.82 |
| 1.19 | -0.099 | +21.69 | 2.39 |
| 1.21 | -0.144 | +18.22 | 2.35 |
| 1.3 | -0.441 | +10.95 | 2.20 |
| 1.4 | -0.939 | +7.87 | 2.07 |

# Uncomplete d(n,p)nn breakup spectra

| $\lambda$ | $\epsilon_{nn}$ [MeV] | $a_{nn}$ [fm] | $r_{eff}$ [fm] |
|---|---|---|---|
| 0.9 | - | -8.25 | 3.12 |
| 1.0 | - | -18.80 | 2.82 |
| 1.19 | -0.099 | +21.69 | 2.39 |
| 1.21 | -0.144 | +18.22 | 2.35 |
| 1.3 | -0.441 | +10.95 | 2.20 |
| 1.4 | -0.939 | +7.87 | 2.07 |

**Changing to positive $a_{nn}$ reduces drastically the magnitude of FSI peak at large outgoing proton energies**

**Integrating large proton energy spectrum one gets angular distribution for n+d → p+dineutron reaction**

**If dineutron exists its energy should be around -100 keV**

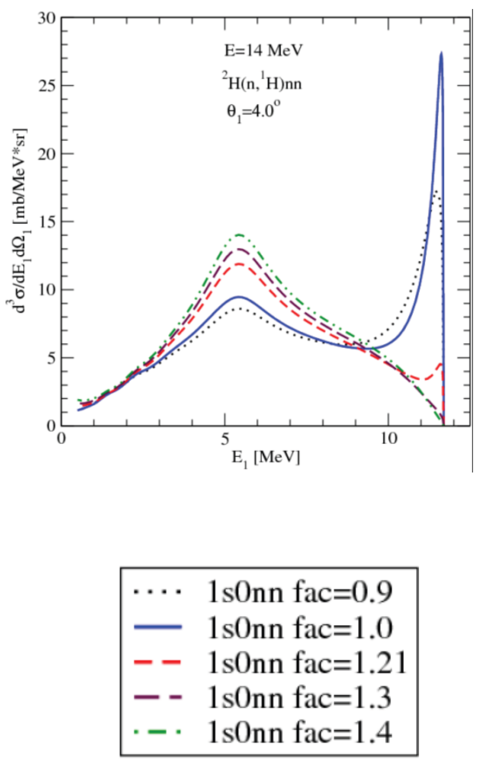


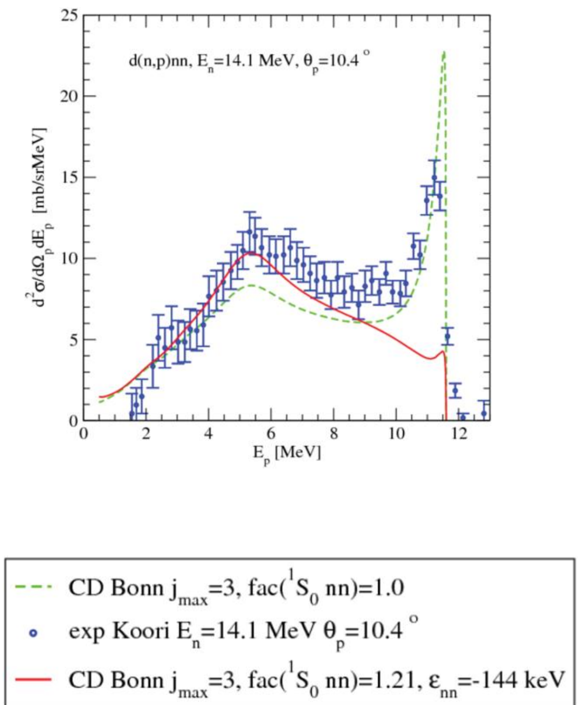


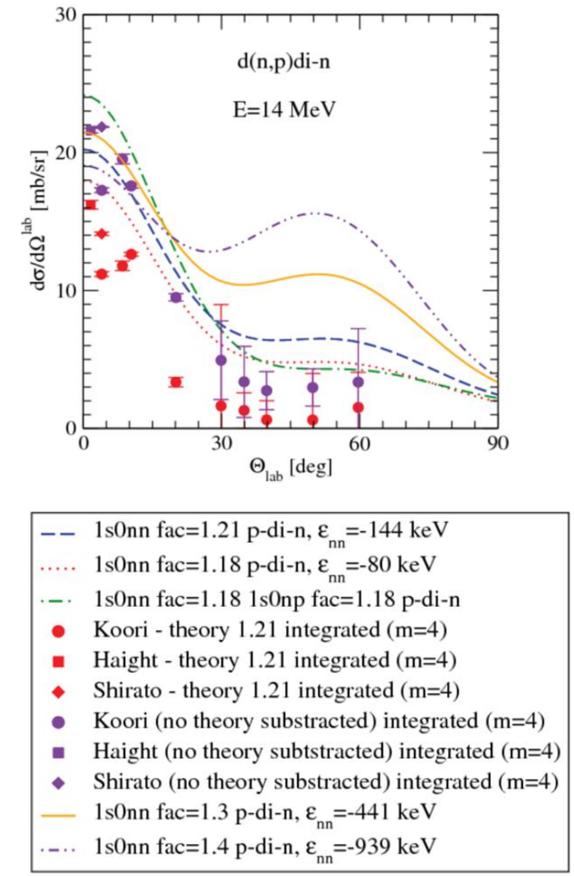

# Where to look for dineutron ?

- It is known that $^3$He is predominantely a spatially symmetric S state with its two protons mainly in opposite spin states. This component amounts for $\approx$ 90% of the $^3$He wave function. Similarily, the two neutrons in $^3$H are restricted to be in a spin-singlet state. That makes the triton target a very suitable tool to look for a nn bound state in $\gamma$ induced breakup of $^3$H. The idea is to measure the spectra of the outgoing protons in such a reaction. The two-neutron bound state, if existant, should reveal itself as a peak above the highest available proton energy from the 3-body decay of $^3$H.

( B. Blankleider …, Phys. Rev. C **29**, 538 (1984)
J.L. Friar ⋯ Phys. Rev. C **42**, 2310 (1990) )

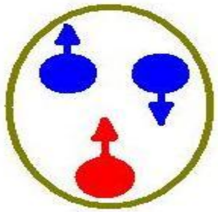

$^3$H

- The big advantage of $\gamma(^3H, p)nn$ reaction is that $\gamma$ interacts predominantely with the proton.

- Also other reactions, such as e.g. $^3$H(n,d)nn and $^3$H(d,$^3$He)nn, provide conditions advantegous for two neutrons to bind. They are complimentary and independent from the $^3$H($\gamma$,p)nn reaction and the data from all three processes should provide an answer to the question whether two neutrons can form a bound state.

# Spectra of outgoing proton from $^{3}H(\gamma,p)nn$ reaction

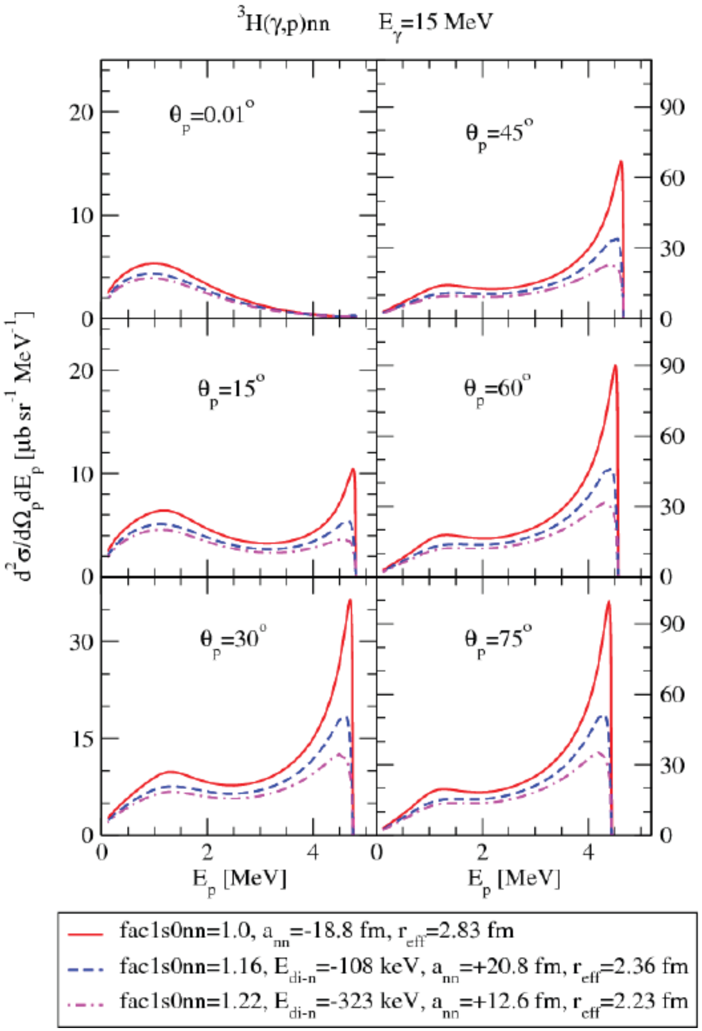


# Lab. angular distributions for $^{3}H(\gamma,n)d$ and $^{3}H(\gamma,p)$dineutron reactions

AV18+MEC

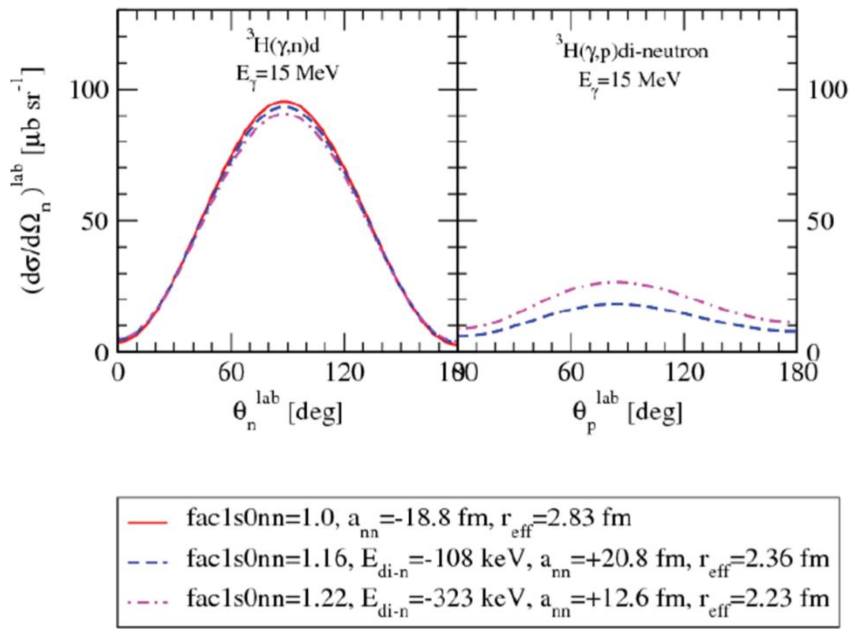

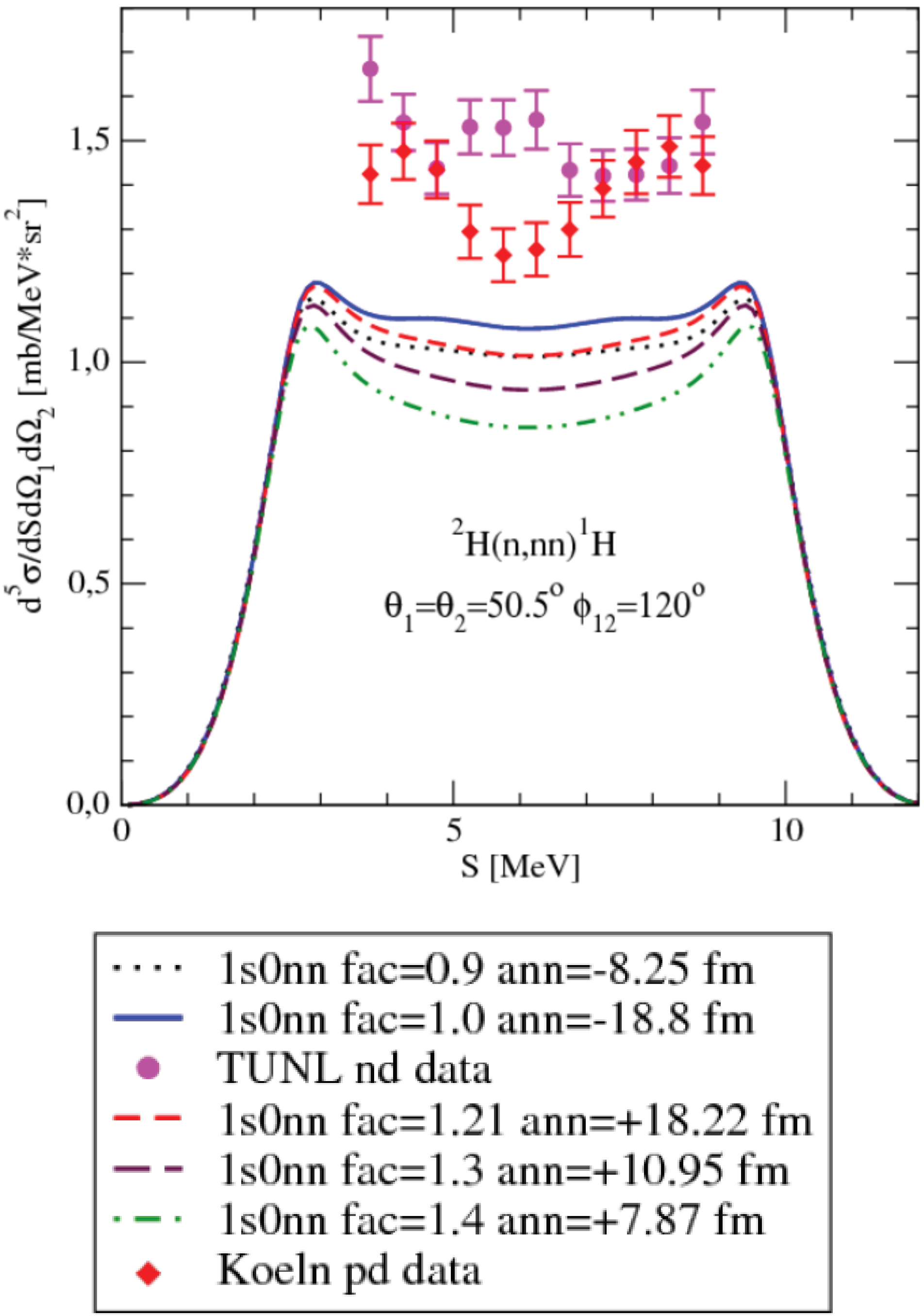


| $\lambda$ | $\epsilon_{nn}$ [MeV] | $a_{nn}$ [fm] | $r_{eff}$ [fm] |
|---|---|---|---|
| 0.9 | - | -8.25 | 3.12 |
| 1.0 | - | -18.80 | 2.82 |
| 1.19 | -0.099 | +21.69 | 2.39 |
| 1.21 | -0.144 | +18.22 | 2.35 |
| 1.3 | -0.441 | +10.95 | 2.20 |
| 1.4 | -0.939 | +7.87 | 2.07 |

- **Dineutron cannot explain nd breakup SST discrepancy !**

- Small 3NF effects at low energies

- Large 3NF effects start to appear at energies above ~ 60 MeV

- Region of large energies seems thus to be the proper one for study 3NF effects

# Higher energy discrepancies

**Elastic scattering d(p,p)d**

NN only (AV18, CD Bonn, Nijm1, Nijm2)

NN+3NF TM99

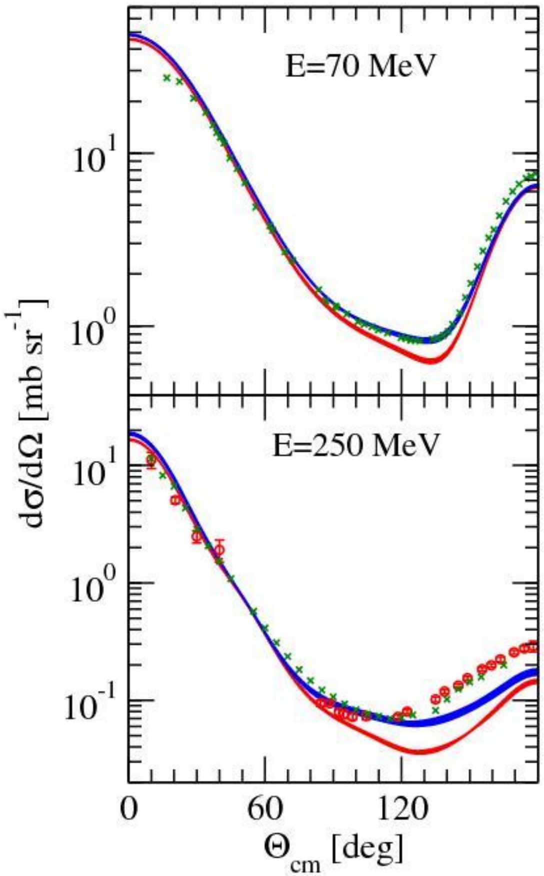


data 70: K.Sekiguchi et al., PR C65, 034003 (2002)

data 250:
x nd – Y.Maeda et al., PR C76, 014004 (2007)
o pd – K.Hatanaka et al., PR C 66, 044002 (2002)

**Total nd cross section:**

- **up to ~ 50 MeV good agreement with predictions based on 2N forces**
- **adding 3NF provides explanation of the disagreement up to ~ 150 MeV**
- **at even larger energies a clear disagreement which increases with energy**

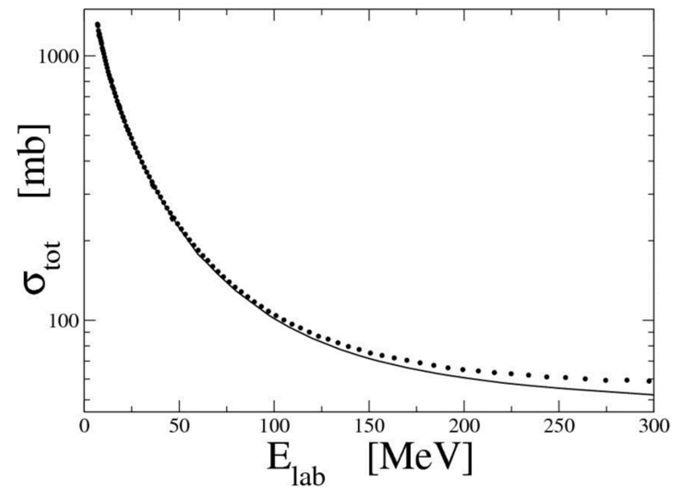


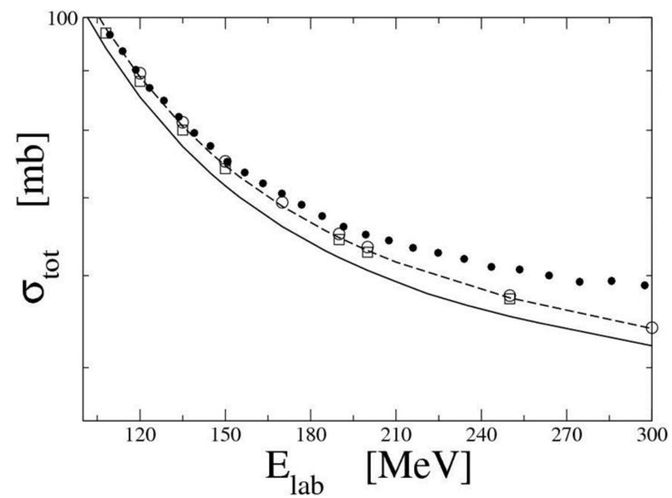

- **what is responsible for large differences between theory and data in 250 MeV cross section and in the total nd cross section even after inclusion of 2π-exchange 3NF ?**

- **it is evident, that in the applied dynamics something is wrong or missing**

- **χPT (and standard meson-exchange picture) provides multitude of additional, short-range components to 3NF (in the meson-exchange picture connected to exchanges of more or heavier mesons), which should be more important with increasing energy**

- **however, increasing energy means also a transition to a region, where relativity could be important → relativistic Faddeev calculations**

# Relativistic Faddeev calculations

( PR C71, 054001 (2005),
PR C77, 034004 (2008),
PR C83, 044001 (2011) )

## The formal structure of the equations remains the same but the ingredients change

- Form of the free Hamiltonian $H_0$ (and $G_0$) changes:

$$H_0 = \sqrt{\left[2\sqrt{m^2 + \vec{k}^2}\right]^2 + \vec{q}^2} + \sqrt{m^2 + \vec{q}^2}$$

- Interacting 2N subsystem (2-3) has nonzero total momentum **-q** in the 3N c.m. system, what leads to the boosted potential V:

$$V(\vec{q}) \equiv \sqrt{\left[2\sqrt{m^2 + \vec{k}^2} + v\right]^2 + \vec{q}^2} - \sqrt{\left[2\sqrt{m^2 + \vec{k}^2}\right]^2 + \vec{q}^2}$$

- V(**q**=0) reduces to the relativistic potential **v** defined in the 2N c.m. system. From V(**q**) the boosted t-matrix is obtained

- The Lorentz transformation from 2N to 3N c.m. is performed along the total momentum of the 2N subsystem, which in general is not parallel to momenta of these nucleons. This leads to **Wigner rotation** of spin states. When defining 3N partial wave states care must be taken about spin states

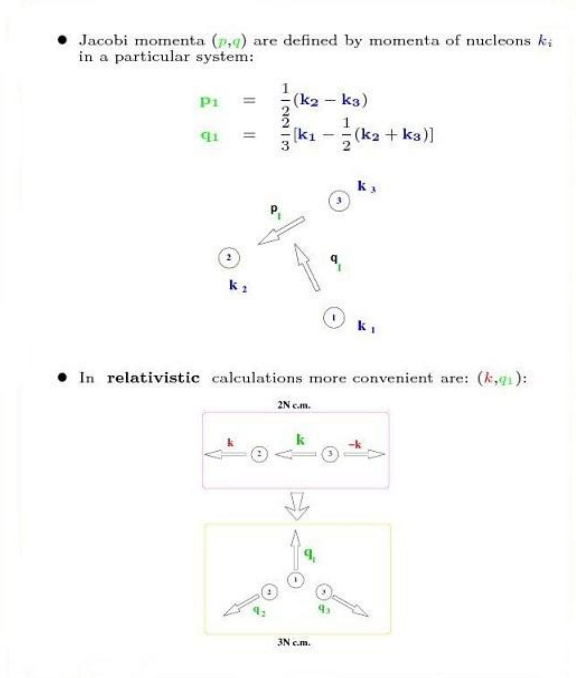

# Only NN interactions:

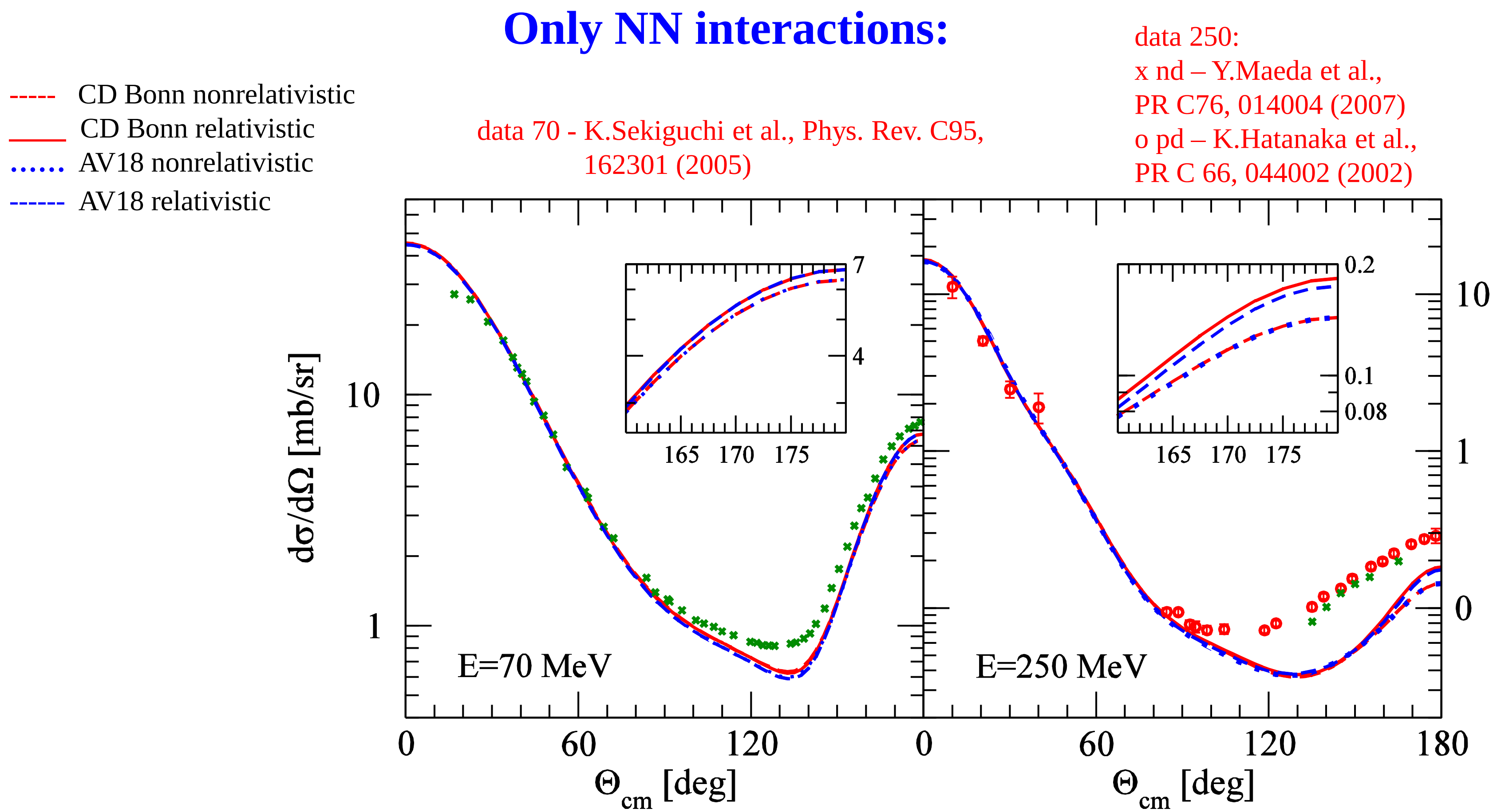


- **effects of relativity seen only in Nd elastic scattering backward cross section !**
- **relativistic effects are not responsible for large discrepancies in elastic Nd scattering cross section**
- **small effects on spin observables**
- **But: what will happen at higher energies when both, 3NF's and relativity, will be treated in a consistent way ?**

(PR C83, 044001 (2011) )

# Faddeev approach with both 3NF and relativity included

## elastic scattering: d(p,p)d

data 135 - K.Sekiguchi et al., Phys. Rev. Lett. 95, 162301 (2005)

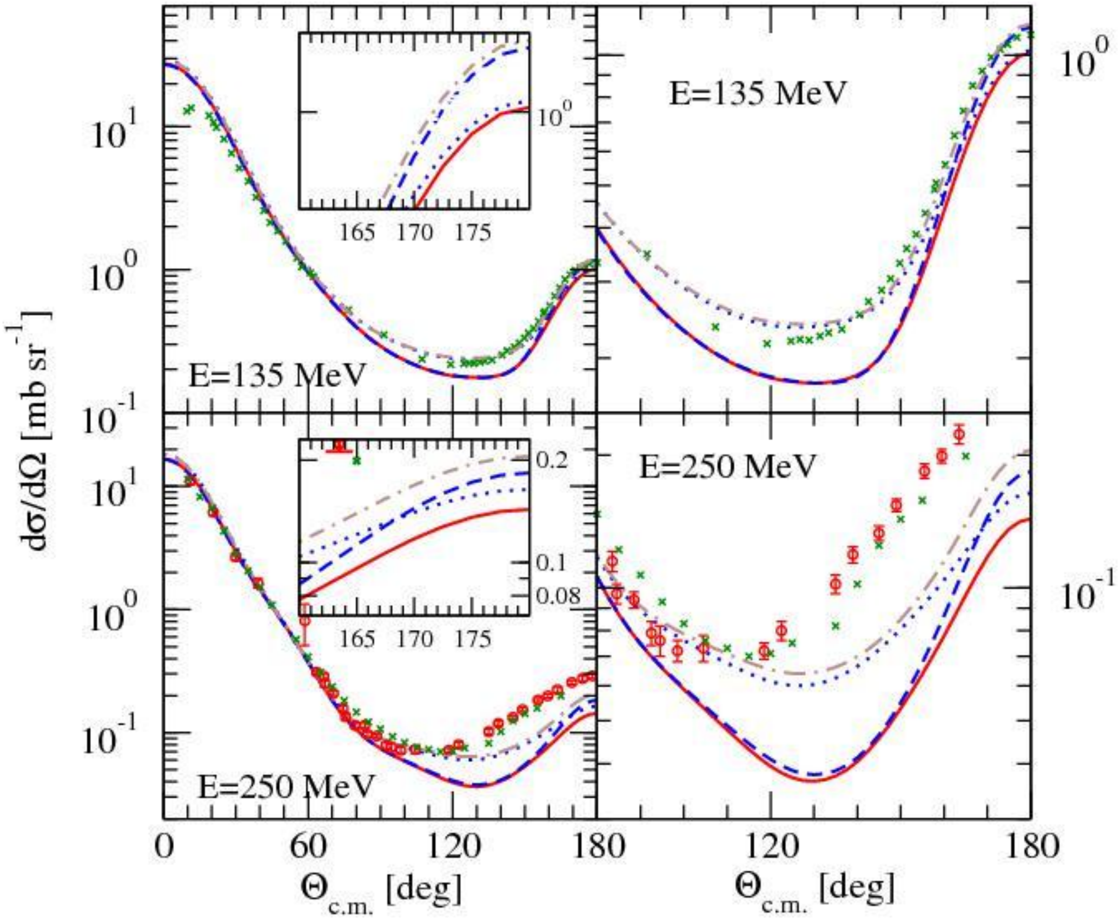


**only NN forces (CDBonn):**

nrel solid red —
rel dashed blue ---

**NN + 3NF (TM99):**

nrel dotted blue …
rel dashed-dotted brown -.-

data 250:
x nd – Y.Maeda et al.,
PR C76, 014004 (2007)

o pd – K.Hatanaka et al.,
PR C 66, 044002 (2002)

- **interplay of relativity and 3NF's leads to slight increase of cross section at angles larger than $\theta_{cm} \sim 100^o$**

- **relativistic effects are not responsible for large discrepancies in elastic Nd scattering**

- **very probably those discrepancies come from neglection of short-range 3NF components, which become active at higher energies**

- **such short-range 3NF's are in the meson-exchange picture given by $\pi$-$\rho$ and $\rho$-$\rho$ exchanges and in $\chi$PT comes a lot of short-range contributions in $N^3LO$ order of chiral expansion (without free parameters)**

# 3NF with $j_{max}$=3 and up to J=3/2 only !

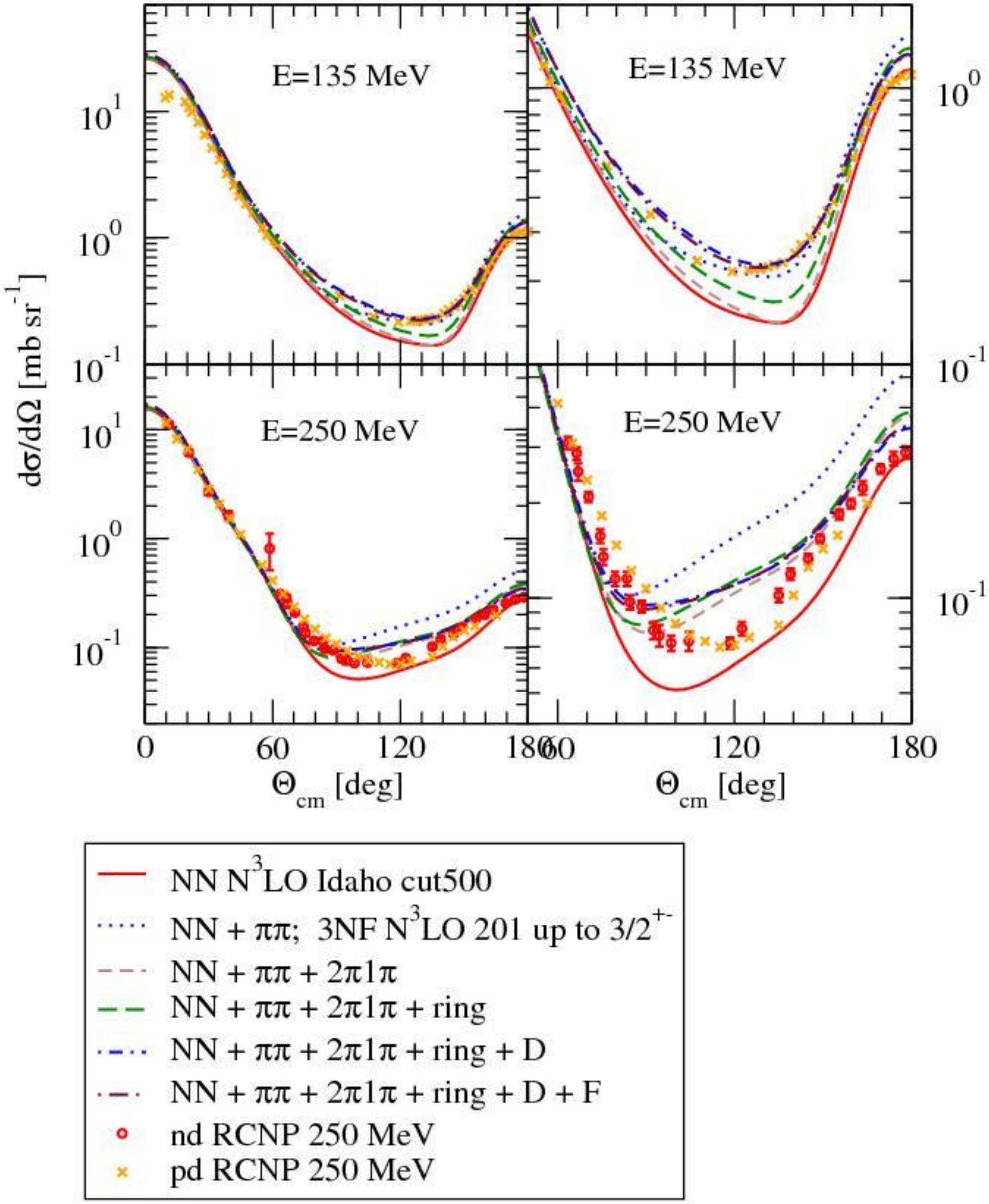

# Challenges:

1) **aPWD will probably fail** to provide required matrix elements of a 3NF: large total angular momenta **j** (in a 2N subsystem) and **J** (of a 3N system) required to get converged results → avoiding PWD and solving Faddeev equations with Jacobi vectors

2) **more work needed in construction of NN $N^3LO$ potentials**:

- dependence on a type of cutoff

- since some terms of $N^3LO$ 3NF depend on low energy constants a covariance analysis of the parameters with respect to the NN experimental uncertainties is required (in spirit of A.Ekstroem et al. , arXiv:1303.4674v1)